Universidade de Aveiro Departamento de Física
2008

Diana Seiça Fidalgo

Monitorização de OSNR e CD baseada em SOAs

Universidade de Aveiro Departamento de Física
2008

Diana Seiça Fidalgo

Monitorização de OSNR e CD baseada em SOAs

Dissertação apresentada à Universidade de Aveiro para cumprimento dos requisitos necessários à obtenção do grau de Mestre em Engenharia Física (2º ciclo), realizada sob a orientação científica do Prof. Dr. José António Luís Jesus Teixeira e do Doutor Rogério Nunes Nogueira, do Instituto de Telecomunicações de Aveiro.

o júri

presidente

Prof. Dr. Manuel Almeida Valente
Professor Associado do Departamento de Física da Universidade de Aveiro

Prof. Dr. José Maria Longras Figueiredo
Professor Auxiliar do Departamento de Física da Faculdade de Ciências e Tecnologia da Universidade do Algarve

Prof. Dr. José António Luís Jesus Teixeira
Professor Auxiliar do Departamento de Electrónica, Telecomunicações e Informática da Universidade de Aveiro

Doutor Rogério Nunes Nogueira
Investigador Auxiliar do Instituto de Telecomunicações

Acknowledgments

I would like to acknowledge my supervisors Prof. Dr. António Teixeira and Prof. Dr. Rogério Nogueira for giving me the chance to work in Optical Communications area and accomplish this project.
I also would like to acknowledge the projects BONE, MOTION, Euro-fos and Sardana to support this project.
I also would like to acknowledge Prof. Dr. Mário Lima for all the constructive hints and discussions held during this work.
I thank a lot Liliana Nicolau and Miguel Drummond for their helpful background on optical communications mainly in the experimental part of the work.
I would like also to acknowledge MsC. João Prata for all support given in the laboratory of Instituto de Telecomunicações - Pólo de Aveiro.
I also like to acknowledge Universidade de Aveiro and Instituto de Telecomunicações - Pólo de Aveiro for the conditions provided.
Finally, I would like to acknowledge my family and friends, who always stand by me.

Palavras-chave

Efeitos Ópticos não lineares, componentes ópticos, medidas ópticas, amplificadores ópticos semicondutores.

Resumo

O presente trabalho tem como objectivo estudar técnicas de monitoria para a razão sinal/ruído e dispersão cromática. Neste estudo consideraram-se duas configurações na monitorização do sinal óptico: amplificador óptico de semicondutor com e sem bomba auxiliar, com o objectivo de avaliar os efeitos *self and cross-phase modulation* neste dispositivo. Para suportar o estudo recorreu-se a simuladores e experiências laboratoriais a ritmos de 40 Gbit/s. Obteve-se um conjunto de directivas para o desenho de filtros para usar nas técnicas referidas.

Keywords Nonlinear optical effects, optical components, optical measurements, semiconductor optical amplifiers.

Abstract The purpose of the present work is to study optical signal-to-noise ratio and chromatic dispersion monitoring techniques. In this study, two configurations in optical signal monitoring were considered: optical semiconductor amplifier, with and without auxiliary pump, in order to evaluate the effects of self and cross-phase modulation in the device. To support the study, simulation work and laboratorial experiments at 40 Gb/s bit rate were performed. A set of directives for the filter design was obtained and used in the referred techniques.

CONTENTS

ACRONYMS

AM	amplitude modulation
ASE	amplified spontaneous emission
ASK	amplitude-shift-keying
CD	chromatic dispersion
CW	continuous wave
DCF	dispersion-compensation-fiber
EDFA	erbium-doped fiber amplifier
FM	frequency modulation
FSK	frequency-shift-keying
FWM	four wave mixing
GVD	group-velocity dispersion
IM/DD	intensity modulation with direct detection
ISI	intersymbol interference
NRZ	nonreturn-to-zero
OA	optical amplifier
OBPF	optical band pass filter
OOK	on-off keying
OSNR	optical signal-to-noise-ratio
PCM	pulse-code-modulation
PM	phase modulation
PMD	polarization mode dispersion
PolM	polarization modulation
PRBS	pseudo-random binary sequence
PSK	phase-shift-keying
RZ	return-to-zero
SMF	single-mode-fiber
SOA	semiconductor optical amplifier
SPM	self-phase-modulation
XPM	cross-phase-modulation

CHAPTER 1

Introduction

1.1. Motivation

Nowadays, optical performance monitoring is essential in dynamic optical networks, since optical signals may cross different paths and different optical components, as a result of routing, add/drop, (de)multiplexing or regeneration procedures which are inherent to reconfigurable networks. They also suffer from non-static degrading effects, which can change with environmental temperature, component drift, aging and fiber plant maintenance. For these reasons, monitoring schemes have to be insensitive to the signal origin and path history [1]. Moreover, the feasibility of implementation of transparent optical networks, where the signals have different bit rates and data formats, depends also on the deployment of enhanced fault management and network maintenance [2]. Furthermore, the increasing complexity of optical networks, where large number of channels, longer transmission distances and high bit rates could be desirable, also justifies the need to implement some mechanism to collect information about signal health. This should be done dynamically and in an automated way [3].

Optical performance monitoring is the solution for this problem and can be defined as the physical layer monitoring of the signal quality, making it available for service providers a way to guarantee quality of signal transmission in optical networks and eventually for network interconnection quality of service guaranty.

High speed conversions to enable measurements on the RF electrical signal is the most straightforward way of achieving the ability to monitor time-domain process necessary to assess information about the transmission impairments, like polarization mode dispersion (PMD), chromatic dispersion (CD) and optical signal-to-noise ratio (OSNR). However, it introduces implementation complexity and high implementation costs, especially for high bit rates. Thus, much research work has been done to uncover new methods for the deployment of desired optical performance monitoring functionalities.

The motivation for the developed work on ambit of this thesis, appears in context of optical signal-to-noise-ratio and chromatic dispersion monitoring based in semiconductor optical amplifier (SOA), for which the reason behind is their ability to amplify and process

optical signals in a wide range of bit rates at modest bias power requirements and in a tiny volume.

1.2. Purpose

The purpose of this work is to find a monitor for optical signal to noise ratio and chromatic dispersion, with high values of monitoring sensitivity and range, at low cost.

1.3. Thesis structure

This present work was divided in 4 chapters, focused in OSNR and CD monitoring. In the first chapter, it was presented the motivation and the purposes of this work. The second chapter presented some theory about, lightwave systems, optical signal degradation and non-linear effects in semiconductor optical amplifiers. In the third chapter was presented the simulation and experimental results for OSNR and CD monitoring. In the fourth chapter was presented the conclusion and future work.

1.4. Contributions

The main contributions of the work described in this thesis, for the knowledge in OSNR and CD monitoring were:

- Study and implementation of an OSNR and CD monitoring technique materialized in publication [4] and submitted to [5].
- Participation in reports for FCT Motion project.

1.5. References

1. Carolina Pinart, Esther Le Rouzic*, Ivan Martinez, "Physical-Layer Considerations for the Realistic Deployment of Impairment-Aware Connection Provisioning", ICTON 2007, pp. 134-137.

2. D. C. Kilper, R. Bach, D. J. Blumenthal, D. Einstein, T. Landolsi, L. Ostar, M. Preiss, A. E. Willner, "Optical Performance Monitoring", J. Lightwave Technol., Vol. 22, No. 1, Jan. 2004.

3. A. Willner, "Self-managing intelligent optical network for smarter, tougher, and cheaper systems", SPIE Newsroom, 2006.

4. D. S. Fidalgo, L. N. Costa, R. Nogueira and A. L. J. Teixeira, “SOA spectral red-shift and blue-shift for OSNR monitoring”, SEON 2008.

5. D. S. Fidalgo, L. N. Costa, R. Nogueira and A. L. J. Teixeira, “Optical Signal-to-Noise-Ratio and Chromatic Dispersion based in SOAs”, Revista DETUA, Vol., No.,2008.

CHAPTER 2

Optical Communications

2.1. Lightwave systems components

The generic block diagram of Fig.1 applies to a fiber-optic communication system, where the communication channel is an optical fiber cable. The optical transmitter and the optical receiver are designed to meet the needs of such a specific communication channel. In this section addressed the general issues related to the role of optical fiber as a communication channel and the design of transmitters and receivers.

Fig1 – Generic optical communication system.

2.1.1. Optical transmitters

The role of an optical transmitter is to convert the electrical signal into the optical domain and to launch the resulting signal into the optical fiber. The Fig.2 shows the block diagram of an optical transmitter. It consists of an optical source, a modulator and a channel coupler. Semiconductor lasers or light-emitting diodes provides many advantages as compared to other light sources when are used as optical sources. Among several advantages, one is their compatibility with the optical fiber communication channel.

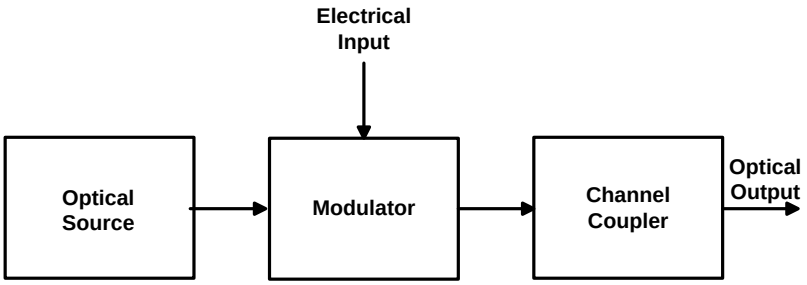

Fig.2 – Components of an optical transmitter.

The optical signal is generated by modulating the optical carrier wave. Although an external modulator is sometimes used, it can be dispensed in some cases, since the output of a semiconductor optical source can be modulated directly by varying the injection current. Such a scheme simplifies the transmitter design and is generally cost-effective; however it brings some limitations for the signal-transmission.

The launched power is an important design parameter. One can increase the amplifier (or repeater) spacing by increasing it, but the onset of various nonlinear effects limits how much the input power can be increased. The launched power is often expressed in dBm units with 1mW as the reference level. The conversion rate is given by,

$$power\,(\mathrm{dBm}) = 10log_{10}\frac{power}{1\,\mathrm{mW}} \quad (1)$$

The launched power is rather low (< -10 dBm) for light-emitting diodes but semiconductor lasers can achieve output powers in the range of 13 dBm. As light-emitting diodes also have some limits in their modulation capabilities, most lightwave systems use semiconductor lasers as optical sources. The bit rate of optical transmitters is often limited by electronics bandwidth rather than by the semiconductor laser itself. With a proper design, optical transmitters can be made to operate at a bit rate of up to 160 Gb/s [1].

2.1.1.1. Modulation formats

The first step in the design of an optical communication system is to decide how the electrical signal would be converted into an optical bit stream. An optical signal could be modulated by applying the electrical signal either directly to the polarization bias current of the optical source or to an external modulator. The Fig.3 shows the relation between rectangular pulse in time domain and its Fourier Transform in frequency domain.

There are two choices for the modulation format of the resulting optical bit stream. These are shown in Fig.4 and are known as the return-to-zero (RZ) and nonreturn-to-zero (NRZ) formats. In the RZ format, each optical pulse representing bit 1 is shorter than the bit slot, and its amplitude returns to zero before the bit duration is over.

In the NRZ format, the optical pulse remains on throughout the bit slot and its amplitude does not drop to zero between two or more successive 1 bits.

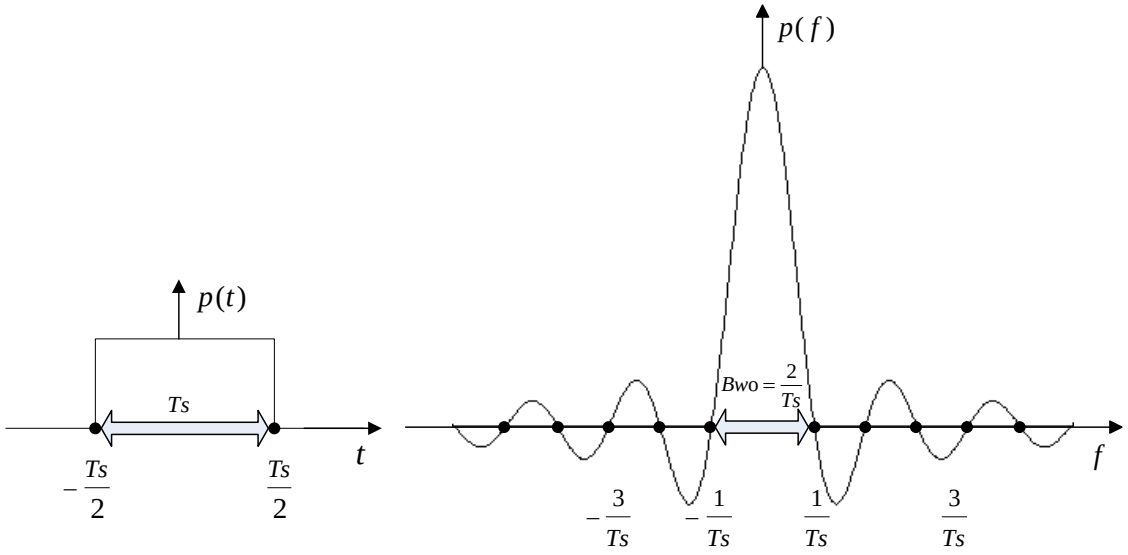

Fig.3 – Relation between rectangular pulse in time domain and its Fourier Transform in frequency domain, where T_s is the time that the pulse is a '1'.

As a result, pulse width varies depending on the bit pattern, whereas it remains the same in the case of RZ format, such as are shown in Fig.5. The time that the bit is a '1' is given by,

$$T_s = \frac{0.33}{B} \tag{2}$$

$$T_s = \frac{0.66}{B} \tag{3}$$

$$T_s = \frac{1}{B} \tag{4}$$

for RZ 33%, RZ 66% and NRZ modulation formats respectively and where B is the bit rate. An advantage of the NRZ format is that the bandwidth associated with the bit stream is smaller than that of the RZ format by about a factor that depends on the RZ duty cycle, simply because the on-off transitions occur fewer times. However, its use requires tighter control of the pulse width and may lead to bit-pattern-dependent effects if the optical pulse spreads during transmission. The NRZ format is often used in implemented systems due to

the above reasons, namely bandwidth.

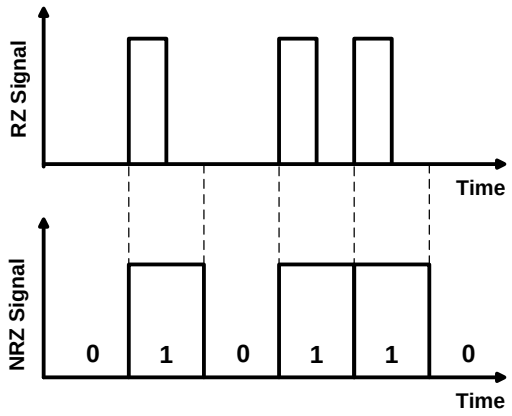

Fig.4 – Digital bit stream 010110…coded by using return-to-zero (RZ 50%) and nonreturn-to-zero (NRZ) modulation formats.

An important issue is related to the choice of the physical variable that is modulated to encode the data on the optical carrier. The optical carrier wave before modulation is of the form [2],

$$E(t) = \hat{e}\mathrm{A}cos(\omega_0 t + \phi) \quad (5)$$

where E is the electric field vector, $\hat{e}$ is the polarization unit vector, A is the amplitude, ω_0 is the carrier frequency, and ϕ is the phase. The spatial dependence of E is suppressed for simplicity of notation. One may choose to modulate the amplitude A, the frequency ω_0, or the phase ϕ. In the case of analog modulation, the modulation schemes are known as amplitude modulation (AM), frequency modulation (FM), phase modulation (PM) and polarization modulation (PolM). The same modulation techniques can be applied in the digital case and are called amplitude-shift keying (ASK), frequency-shift keying (FSK), and phase-shift keying (PSK), depending on whether the amplitude, frequency, or phase of the carrier wave is shifted between the two levels of a binary digital signal. The simplest technique consists of simply changing the signal power between two levels, one of which is set to zero, and is often called on-off keying (OOK) to reflect the on-off nature of the resulting optical signal. Most digital lightwave systems employ OOK in combination with a pulse-code modulation (PCM).

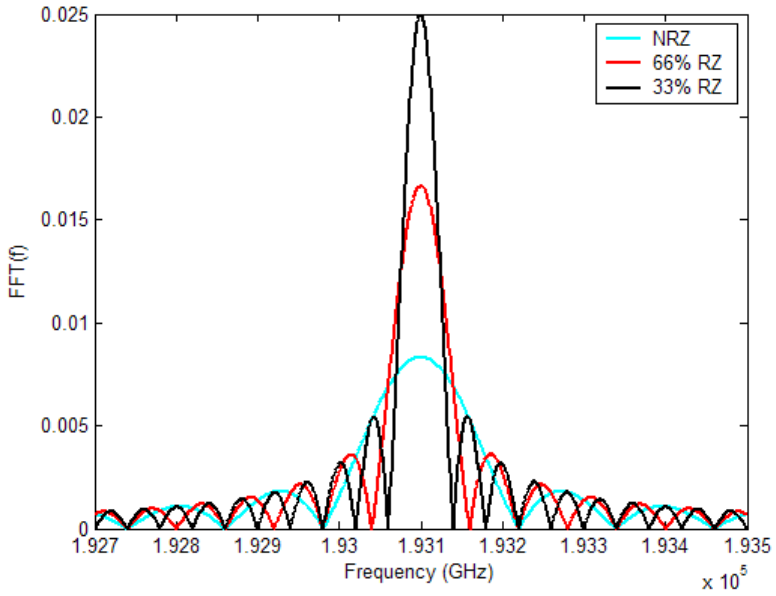

Fig.5 – Fourier Transform of a rectangular pulse for three modulation formats, NRZ (blue), 66% RZ (red) and 33% RZ (black).

2.1.2. Optical receivers

An optical receiver converts the optical signal received at the output end of the optical fiber into the proportional electrical signal. Fig.6 shows the block diagram of an optical receiver. It consists of a photodetector and a demodulator. The design of the demodulator depends on the modulation format used by the lightwave system. Most lightwave systems employ a scheme referred to as "intensity modulation with direct detection" (IM/DD). Demodulation in this case is done by a decision circuit that identifies bits as 1 or 0, depending on the amplitude of the electric signal. Optical receivers can be made to operate at a bit rate of up to 160 Gb/s [1].

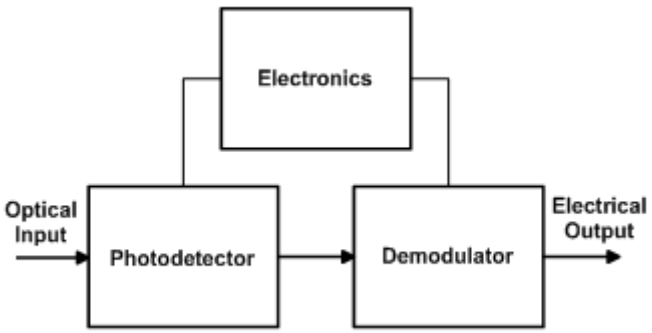

Fig.6 – Components of an optical receiver.

The accuracy of the decision circuit depends on the SNR of the electrical signal generated at the photodetector.

2.1.3. Optical fibers as a communication channel

The role of a communication channel is to transport the optical signal from transmitter to receiver without distorting it. Most lightwave systems use optical fibers as the communication channel because silica fibers can transmit light with losses as small as 0.2 dB/km. Even then, in those apparently good conditions, optical power reduces to only 1% after 100 km [3]. For this reason, fiber losses remains an important design issue and determines the repeater or amplifier spacing of a long-haul lightwave system. Another important design issue is fiber dispersion, which leads to broadening of individual optical pulses with propagation. If optical pulses spread significantly outside their allocated bit slot, the transmitted signal is severely degraded due to intersymbol interference. Eventually, it becomes impossible to recover the original signal with accuracy. In this way, most optical communication systems use single-mode-fibers, since this problem is becomes even more severe in the case of multimode fibers, since pulses spread rapidly (typically at a rate ~10 ns/km) because of different speeds associated with different fiber modes. Material dispersion, related to the frequency dependence of the refractive index, still leads to pulse broadening (typically < 0.1 ns/Km) [3], but it is small enough to be acceptable for most applications and can be reduced further by controlling the spectral width of the optical source. However, material dispersion limits the bit rate and the transmission distance of fiber-optic communication systems.

2.2. Optical signal degradation

2.2.1. Chromatic dispersion

Chromatic dispersion arises from the frequency dependence of the refractive index of an optical fiber, which induces different spectral components of the propagation optical pulses to travel at different speeds at an optical link, causing pulse broadening, which in turn leads to intersymbol interference (ISI) in the received signal and to a reduction of the system performance.

The intermodal dispersion in multimode fibers leads to considerable broadening of short optical pulses ~10 ns/km. In the geometrical-optics description, such broadening is attributed to different paths followed by different rays. In the modal description it is related with the different mode indices (or group velocities) associated with different modes. The main advantage of single-mode fibers is that intermodal dispersion is absent simply because the energy of the injected pulse is transported by a single mode. However, pulse broadening does not disappear altogether. The group velocity associated with the fundamental mode is frequency dependent because of chromatic dispersion. As a result, different spectral components of the pulse travel at slightly different group velocities, a phenomenon referred to as group-velocity dispersion (GVD), intramodal dispersion, or simply fiber dispersion. This phenomenon is illustrated in Fig.7.

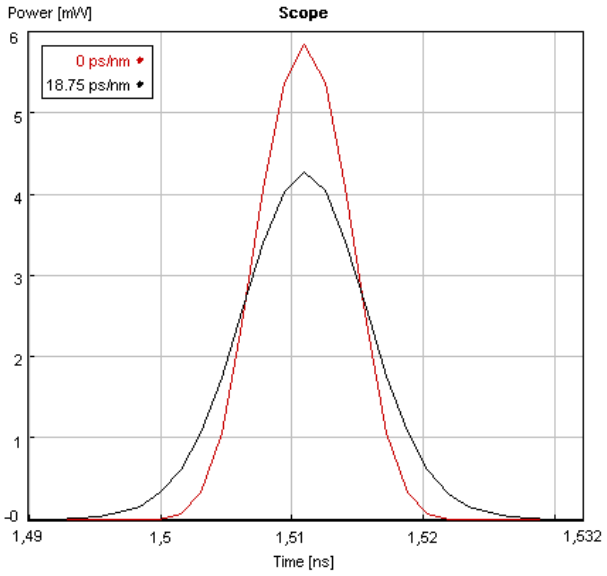

Fig.7 – Illustration of pulse broadening: optical pulse amplitudes for zero dispersion (red) and 18.75 ps/nm accumulated dispersion (black) for RZ 33% and with 80 GHz of bandwidth.

If considering unchirped optical pulses at the input of an optical fiber and first-order group velocity dispersion, the dispersion exhibits a linear behavior. For the normal regime, with positive GVD, the pulses experience negative chirp at the leading-edge and positive chirp at the trailing-edge. This is the same as saying that, in the normal dispersion regime, the red components of a propagating pulse travel faster than its blue components. Oppositely, for anomalous dispersion regime, with negative GVD, a propagating pulse

exhibits positive chirp at the leading-edge and negative chirp at the trailing-edge. The description of chirp profiles for both positive and negative GVD cases is illustrated in Fig.8.

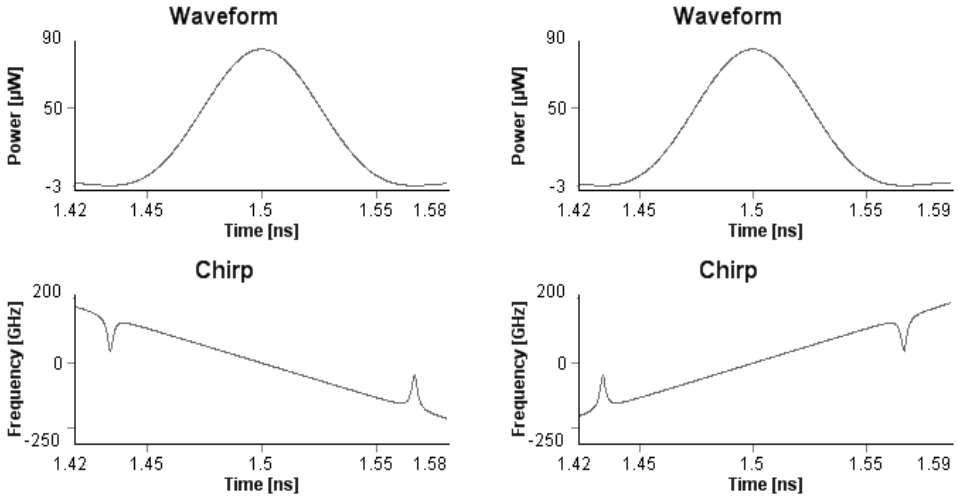

Fig.8 – Pulse amplitude and chirp for positive GVD (left) and negative GVD (right).

The dispersion parameter or dispersion coefficient for an optical fiber is defined as [4]:

$$D = \frac{d\beta_1}{d\lambda} = -\frac{2\pi c}{\lambda^2}\beta_2 \tag{6}$$

where c is the light velocity at vacuum, λ is the operating wavelength and β_2 is the GVD parameter which represents dispersion of the group velocity and is expressed in ps^2/m or equivalently DL in ps/nm/km. The accumulated dispersion along the fiber can be also determinate by the parameter group-delay, denoted by $\Delta\tau$, which is defined as the difference in propagation time between two eigenmodes [5].

$$D_{accumulated} = \frac{d\Delta\tau}{d\lambda} \tag{7}$$

In optical communication systems, the pulse width of the optical pulses transmitted over a fiber is determined by the bit rate, B of the system. If the pulses spread over its designated bit slot, given by $T_s = 1/\mathrm{B}$ for the case NRZ modulation format, as a

consequence of dispersion induced broadening, pattern dependent detection errors will occur and so a given value for the bit rate can be associated with a transmission distance limit. Usually the transmission capacity of an optical link is given by the product of the bit rate with the distance.

On the other hand, the optical transmission capacity can be related to the spreading of the optical pulses that travel along the fiber,

$$\Delta T_s < \frac{1}{B} \tag{8}$$

where B is the bit rate, which is the same as assuming that the pulse spreading should be lower than the bit period. This is a simple rule of thumb, which defines the transmission limit BL, where L is the length of the optical fiber as:

$$B.\Delta T_s < 1 \Leftrightarrow B.L.|D|.\Delta\lambda < 1 \Leftrightarrow L < \frac{1}{B.|D|.\Delta\lambda} \Leftrightarrow L < \frac{c}{2B^2.|D|.\lambda^2} \tag{9}$$

where

$$2B \cong \Delta f \approx \frac{c}{\lambda^2}\Delta\lambda \tag{10}$$

So, for the case of an external modulator without chirp, the limiting condition imposed by GVD is:

$$L < \frac{c}{2B^2.|D|.\lambda^2} \Leftrightarrow GVD_{max} = \frac{c}{2B^2.\lambda^2} \tag{11}$$

where L is the length of the fiber, λ is the operating wavelength, B is the bit rate and D is the dispersion coefficient.

According to the equation 11, for channel wavelength located in the third-window around 1550 nm, the unambiguous maximum dispersion range is about 60 ps/nm for 40 Gb/s system [6].

2.2.2. Optical signal-to-noise-ratio

OSNR is often used as an indicator for the signal quality and is defined as the ratio of the signal power at the peak of a channel to the noise power interpolated at the position of the peak and is described by the following equation [7],

$$OSNR = 10 \times log \frac{P_i}{N_i} \tag{12}$$

where P_i is the optical signal power in watts at the ith channel, and N_i is the interpolated value of noise power in watts in a defined optical bandwidth.

Although the out-of-band noise can be suppressed by the filtering effects of the multiplexers/demultiplexers components, it is the in-band amplified spontaneous emission (ASE) noise that mainly determines the optical-signal-to-noise-ratio (OSNR) [8].

2.3. Semiconductor optical amplifiers

The development of SOAs is closely related to that of semiconductor lasers. The first devices were normal laser diodes biased bellow threshold. In 1966 the use anti-reflection coatings was proposed to reduce the optical feedback and allow amplification of infrared light. The double heterostructure was demonstrated in 1969 [9] and led to significant improvements both in lasers and SOAs. Whilst first studies focused on the 830 nm range, in the 80's decade InP/InGaAS SOAs were designed to operate in the 1300 nm and 1550 nm regions [10]. By the second half of the 80's the first transmission tests employing SOA as in-line amplifiers were reported.

By 1987 the Erbium Doped Amplifier (EDFA) was invented and stirred the attention from the SOA for linear amplification purposes. By mid 90's the first devices featuring high gain and saturation power, and low polarization dependence were reported [11].

2.3.1. SOA Operation

A SOA is very similar to a semiconductor laser without, or with negligible optical facet feedback. An incoming signal injected into the SOA, propagates along its optical

waveguide and is amplified by stimulated emission. The optical gain is achieved by inverting the carrier population in the active region via electrical pumping.

All the different SOA structures available today are based on a semiconductor p-n junction [12]. The SOA requires forward biasing of the p-n junction, which allows the diffusion of electrons and holes across the junction, also known as depletion region. These can recombine through radiative or nonradiative mechanisms. Three radiative mechanisms are possible in the semiconductor: absorption, stimulated emission, and spontaneous emission. The absorption is a loss process and the stimulated emission is the mechanism responsible for the optical gain. The spontaneous emission originates photons with random phase and frequency and that effect is essentially noise which contributes to reduce the optical gain.

2.3.2. SOA versus other optical amplifier types

The SOA is not the only optical amplifying device used in fiber communications. Other kinds of optical amplifiers exist. It is not possible a priori to say which amplifier is the best, because it depends on the particular application.

An ideal amplifier should feature constant gain, regardless of the input signal power. However, the gain of all optical amplifiers saturates for high power input signals, resulting in different gains for input signals with different power values. This effect is called gain saturation and an example is shown in Fig.9.

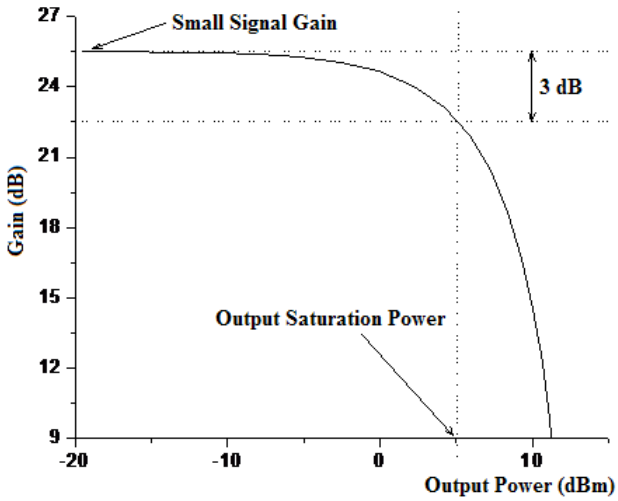

Fig.9 – Example of gain and output power saturation in the SOA.

In an EDFA the gain dynamics has response times in the order of the milliseconds, consequently the optical gain varies with the average power of the signal, resulting in negligible inter and intra channel distortion.

In a SOA, the gain dynamics are reasonably fast, in the order of the tens of picoseconds, value comparable to the pulse duration in current systems. This result in: intra channel patterning effects, due to the time scales of gain compression; inter channel interference; and newly generated frequencies, due to non-linearities, e.g. Four Wave Mixing (FWM). Also phase modulation occurs in the SOA due to variations of the refractive index with the input power.

From the previous considerations, it can be concluded that when SOA is used as linear amplifier, the input signal power must be carefully chosen, to prevent the undesired distortion effects. On the other hand, the fast gain and phase dynamics can bring additional features for non-linear applications.

The advantages of SOAs are their versatility and monolithic integrability with other optical components (like passive waveguides and couplers) to perform more complex functions. They are compact, electrically pumped and have a large optical bandwidth. Moreover, they allow a wide flexibility in the choice of the gain peak wavelength. In non-linear operation they can perform all-optical signal processing because of their strong nonlinearities and their fast dynamics. Finally, due to all above, they are potentially cheap.

In the case of linear operation, i.e. as preamplifiers, boosters, or in-line amplifiers, SOAs show inferior performances than fiber amplifiers like EDFAs. In systems which require very good amplifier performances (as in long-haul transmission) almost always fiber amplifiers are used. However, in local and metropolitan networks less performance and low-cost linear amplifiers can be tolerated. Because of the economical aspect, SOAs are very interesting for these applications [13].

2.3.3. Applications

SOAs have many applications,

- Linear Amplifier;
- Modulator and receiver;
- Wavelength Conversion;
- Self and Cross Gain Modulation

- Self and Cross Phase Modulation;
- Four Wave Mixing
- Cross Polarization Rotation

2.3.3.1. Self and cross phase modulation

SPM is the modulation of the output signal phase caused by refractive index changes induced by the power variations of the same signal. Because the refractive index of SOA changes with the gain saturation when the signal is amplified, it will induce a phase change in the signal being amplified, as shown in the Fig.10 (right). If more than one signal is being simultaneously amplified, there will be XPM between the signals, as illustrated in the Fig.11 (right). Since the XPM only affects the phase, it is necessary to perform a phase modulation to amplitude modulation conversion in order to have the required amplitude information at the converted signal wavelength.

Based in these two non linear effects monitoring of optical signal to noise ratio and chromatic dispersion can be achieved as it is going to expressed in the next sections.

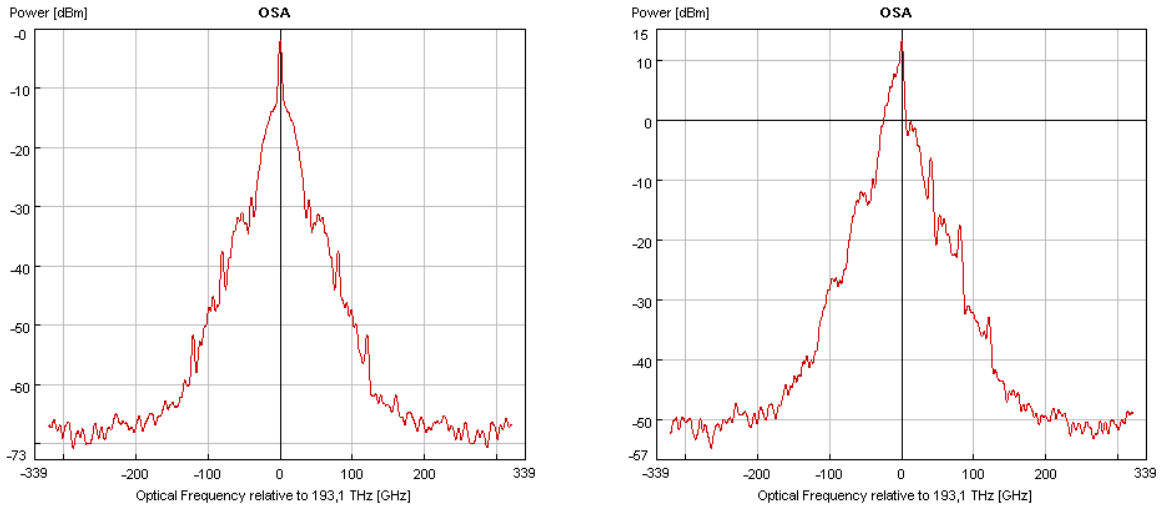

Fig.10 – Output spectrum before SOA (left) and after SOA (right) for SPM without pump and NRZ modulation format.

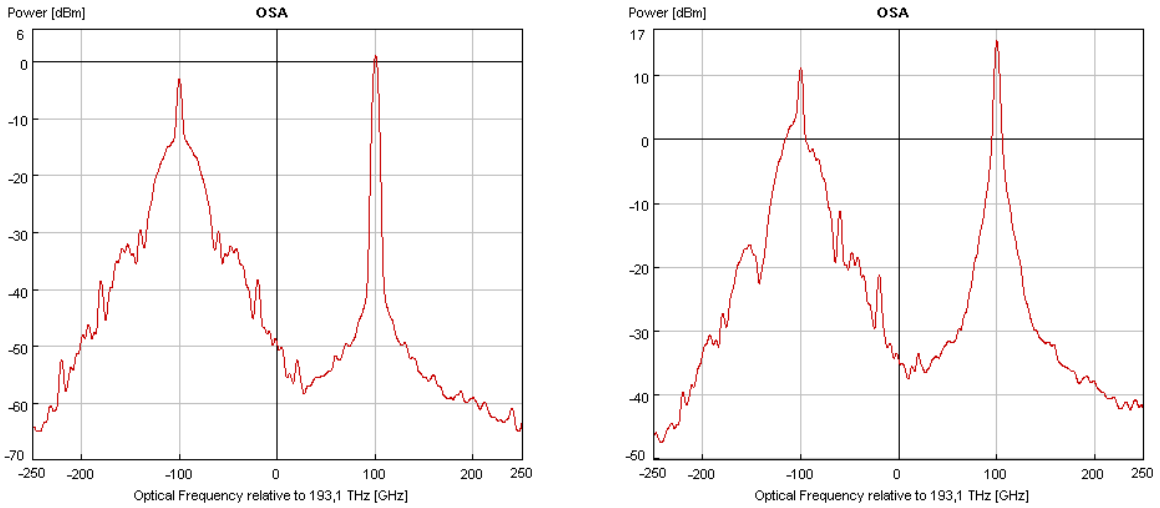

Fig.11 – Output spectrum before SOA (left) and after SOA (right) for SPM with pump (left spectrum) and XPM (right spectrum) for NRZ modulation format.

2.4. CD and OSNR monitoring using SOAs

Some research work has been made focusing on the spectral broadening occurring in a semiconductor optical amplifier has a consequence of CD and OSNR [14, 15]. All methods simply establish a relationship between the average power of the red-shift portion of the spectrum at the output of the SOA and the accumulated dispersion and optical signal to noise ratio suffered by an optical signal when transmitted through an optical fiber.

The two main physical mechanisms occurring in the SOA, which need to be considered, are:

- Spectral broadening occurring in a SOA induced by self-phase modulation (SPM) mechanism due to nonlinear gain saturation process;
- Cross-phase modulation (XPM) due to refractive index changes induced by the data signal which affect the output phase of the continuous wave (CW) pump signal propagation through the SOA.

Considering the amplification process occurring in a SOA, it is influenced by nonlinear mechanisms arising from gain saturation that causes distortion of the pulses, since the leading-edge of the arriving pulse reduces the available gain for the trailing-edge. This saturation mechanism depends strongly on the power of the pulses and can result into pulse compression or broadening, depending on the operation conditions [16]. So, it is expected

that the spectral shift towards the long-wavelength side, also known as red-shift, depends largely on the input pulse power and on the amplifier gain.

The nonlinear mechanism of SPM in the SOA makes it possible to correlate the red-shifted portion of the optical power at its output with the amount of chromatic dispersion induced by the fiber and the OSNR. Thus, by simply taking a measure of the power of a low frequency side of the spectrum at the output of the SOA, it is possible to monitor the degree of accumulated dispersion and the OSNR on the optical signal.

2.5. References

1. http://www.hecto.eu/

2. G. P. Agrawal, "Fiber-Optic Communication Systems", 3rd Ed.,Wiley-Interscience, pp.13-15, 2002.

3. G. P. Agrawal, "Fiber-Optic Communication Systems", 3rd Ed.,Wiley-Interscience, pp.17, 2002.

4. G. P. Agrawal, "Nonlinear Optical Fibers", 3rd Ed., Optics and Photonics, Academic Press, 2001.

5. S. Bette, C. Caucheteur, M. Wuilpart and P. Mégret, "Spectral Characterization of differential group delay in uniform fiber Bragg gratins, Optics Express, Vol.13, No.25, December 2005.

6. R. Gaudino, "Transmitter Optimization and Theoretical Bounds for Dispersion-Limited Optical Fiber Links", IEEE Trans. Comm., Vol.52, No.9, Sep.2004.

7. Daniel Gariépy, Gang He, "Measuring OSNR in WDM Systems-Effects of Resolution Bandwidth and Optical rejection Ratio", Application Note 098, EXFO, 2005.

8. Xiangqing Tian, Yikai Su, Weisheng Hu, Lufeng Leng, Peigang Hu, Hao He, Yi Dong and Lilin Yi, "Precise In-Band OSNR and Spectrum Monitoring Using High-Resolution Swept Coherent Detection", IEEE Photonics Technology Letters, Vol.18, No.1, Jan.2006.

9. I. Hayashi, M. Panish, P. Foy, "A low-threshold room-temperature injection laser", IEEE J. Quantum Electron., Vol.5, No.4, pp.211-212, Apr.1969.

10. J. Simon, "GaInAsP semiconductor lasers amplifiers for single-mode fiber communications", J. Lightwave Technol., Vol.5, No.9, pp.1286-1295, Sept.1987.

11. C. Holtmann, P. A. Besse, T. Brenner, H. Melchior, "Polarization independent bulk active region semiconductor optical amplifiers for 1.3 μm wavelengths", IEEE Photon. Technol. Lett., Vol.8, No.3, pp.343-345, Mar.1996.

12. G. Agrawall, N. Dutta, "Semiconductor Lasers", New York, Van Nostrand Reinhold, 2nd Ed., 1993.

13. Lorenzo Occhi, "Semiconductor Optical Amplifiers made of Ridge Waveguide Bulk InGaAsP/InP: Experimental Characterization and Numerical Modeling of Gain, Phase, and Noise", Ph.D.thesis, ETHZ, Zurich, 2001.

14. P. Vorreau, D. C. kilper, J. Leuthold, "Optical Noise and Dispersion Monitoring With SOA-Based Optical 2R Regenerator", IEEE Photon. Technol. Lett., Vol.17, No.1, Jan.2005.

15. Y. Shi, M. Chen, S. Xie, " A novel low power chromatic dispersion monitoring technique employing SOA spectral shift", Optics Communications, Vol.230, pp.297-300, Nov.2003.

16. D. C. Kilper, R. Bach, D. J. Blumenthal, D. Einstein, T. Landolsi, L. Ostar, M. Preiss, A. E. Willner, "Optical Performance Monitoring", J. Lightwave Technol., Vol.22, No.1, Jan.2004.

CHAPTER 3

Simulation and Experimental Results

3.1. Simulation and experimental setup

One of the configurations used to test experimentally the methodology is based on the one presented in [1]. As shown in Fig.12, the data signal enters the SOA input after propagating through a residual dispersion rack, composed of several small spans of single-mode fiber (SMF) and dispersion compensation fiber (DCF), which can be combined to induce positive or negative accumulated dispersion respectively within the range of $\pm 60\ ps/nm$ in simulations and experiments. On the other hand for OSNR monitoring, the residual dispersion rack is disconnected and a noise source, filtered EDFA is added to the data signal to allow controlling the OSNR. The noise power source was varied to obtain an OSNR range between 6 dB and 30 dB in simulations and between 14 dB and 30 dB in experiment. OSNRs lower than 6 dB are not of interest for the targeted applications transmission, due to low performance. It was not possible to achieve in laboratory OSNRs lower than 14 dB, due to noise source power limitation.

At the output of the SOA, the signal is band-pass filtered to obtain a specific portion of the spectrum and its average power, then measured by an ideal photodiode (PIN), allowing the CD and OSNR to be determinate. The optical band-pass filter (OBPF) is detuned along wavelength from the data central wavelength.

Another configuration used for the simulation work is based on the one proposed in [2], in which the data signal is coupled at the input of the SOA with CW pump by using a 3-dB coupler. Two different monitoring signals can be obtained by filtering the spectrum portion of the SPM signals or XPM signals at the output of the SOA. The configuration setup is shown in Fig.13.

The results are obtained for transmitted data signal with 33% and 66% duty-cycle RZ and NRZ data format with infinite extinction ratio at 40 Gb/s bit rate, with a pseudo-random binary sequence (PRBS) of 2^7-1 bits in simulations and with 2^{31}-1 in experiment. The data signal frequency for the first configuration is $193.1\ THz$ for simulation and $193.3\ THz$ for experiment. The data and pump signals frequency for the second configurations are $193.0\ THz$ and $193.2\ THz$ for simulation and $193.3\ THz$ and

193.5 THz for experiment respectively. The data and pump signals are 200 GHz spaced, as way these signals do not overlap. The data and pump signal frequency central are different for simulations and experiments, due to the central frequency channel limitations of multiplexer and de-multiplexer used to filter to the noise.

The SOA has an output saturation power of 6 dBm and is set to operate with 200 mA bias current.

For the first simulation configuration, the data signal enters the SOA with a constant power of 0 dBm and for the second configuration, the data power is 2 dBm and the CW power is 4 dBm. The data signal and pump signal power values are maintained constant by using an ideal optical amplifier (OA). The optical amplifier is not used in experimental setup and as a consequence it is impossible to adjust the data signal power. The data signal power corresponds to -8.78 dBm and pump signal power to -6.78 dBm.

The simulation results are obtained by VPI simulator.

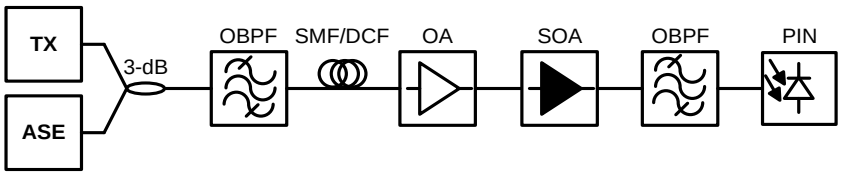

Fig.12 – Configuration for CD and OSNR monitoring signal based on SPM spectrum without CW pump.

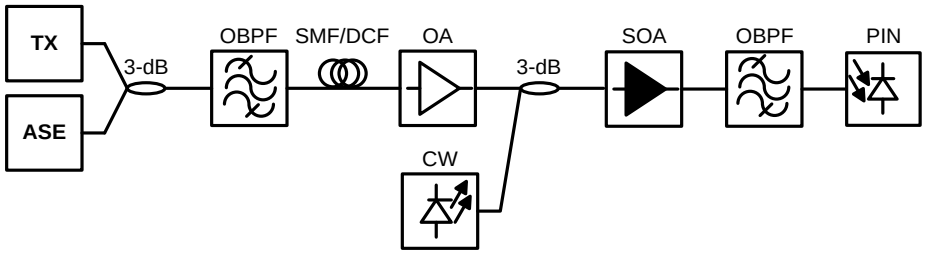

Fig.13 – Configuration for CD and OSNR monitoring signal based on SPM spectrum with CW pump and XPM spectrum.

3.1.1. Optimization of the optical filter

A set of simulations were performed in order to optimize the optical filter as a way to improve the quality of the monitoring signal. For the two configurations, it was made an evaluation of the influence of the data and pump powers, along with the optimization of

optical filters. To choose the dispersion range, first was applied a methodology described by Fig.14. For cases with behavior similar to this, i.e., the curve do not present a trend well defined, it was considered two ranges, in which the signal power decreases with the dispersion increases. It was applied a condition, that only allows dispersion ranges higher than 10 ps/nm for simulations and 3.5 ps/nm for experiment. For this particular case, the range 2 satisfies the impost condition. Thus, only the values within the range 2 are considerate for the next step. The OSNR monitoring do not need this step, because the

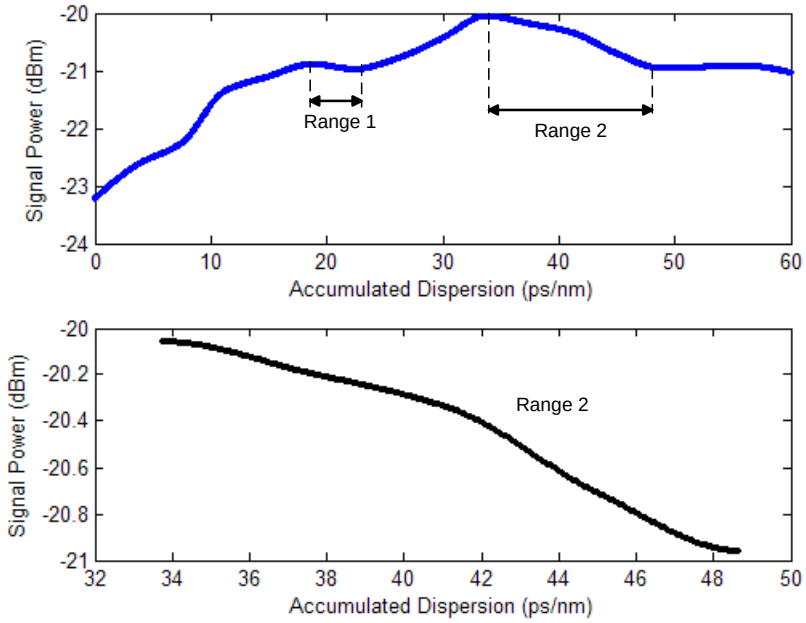

Fig.14 – Illustration of the total values of monitoring signal power (up) and the values belonging to range 2 (down).

curve behavior presents a trend well defined, i.e., the optical noise power decreases with OSNR increases.

The second step consists in application of merit figures. The figures of merit used are the monitoring range and the monitoring sensitivity. For CD, monitoring range is defined as the maximum detectable CD within 10% and 90% of the monitoring signal power change, and monitoring sensitivity is defined as the change in dB of the monitoring signal corresponding to a change of 1ps/nm of accumulated dispersion. For OSNR, monitoring range is defined as the maximum detectable OSNR within 10% and 90% of the monitoring signal power change, and monitoring sensitivity is defined as the change in dB of the monitoring signal corresponding to a change of 1 dB of OSNR. It was also established the

minimum CD and OSNR. The Fig.15 illustrates an example of the interval of considered values for sensitivity and range calculating.

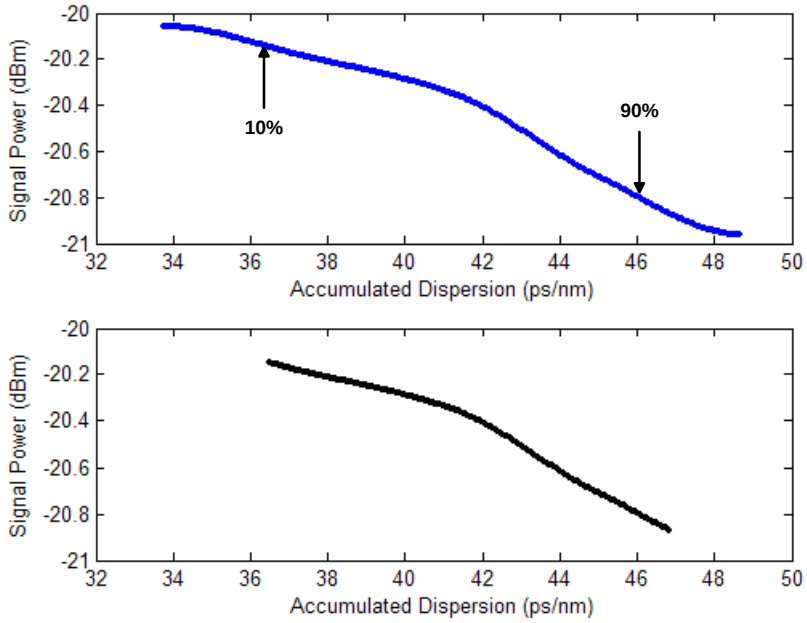

Fig.15 – Illustration of the total values of monitoring signal power (up) and the values of monitoring signal between 10% and 90% (down).

The equations (13) and (14) correspond to sensitivity and range calculating for the case of dispersion monitoring, where P is the monitoring signal power and D is the accumulated dispersion.

$$\text{Sensitivity} = \frac{P(10\%) - P(90\%)}{Range} \tag{13}$$

$$Range_{Dispersion} = D(10\%) - D(90\%) \tag{14}$$

The first step illustrated in Fig.14 was made to achieve better compromise between dispersion range monitoring and power sensitivity. The second step illustrated in Fig.15 was done to obtain a better curve trend.

Higher values of detected power, which are less sensitive to noise, are obtained by placing the filter closer to the central part of the spectrum, at the expense of decrementing

the monitoring signal sensitivity because of the inclusion of some power from that central part of the spectrum, derived from the finite response of the filter. But putting the filter too far away from the central part or choosing a narrower filter could result in severe degradation of the monitoring sensitivity due to noise influence. Hence a mid-term solution had to be found by optimizing both the bandwidth and detuning of the optical filter.

The second order Gaussian filter was the optical filter used, and it was detuned along the frequency. The transfer function of this filter is given by [3],

$$H(s) = e^{-\ln\left(\sqrt{2}|S_{BP}|^{2n}\right)} \tag{15}$$

where n is the filter order and S_{BP} for band pass filter is given by,

$$S_{BP} = 2\frac{\omega - \omega_0}{\omega_p} \tag{16}$$

where ω is the frequency, ω_0 the central frequency and ω_p the bandwidth of optical filter.

The monitoring signals obtained show the monitoring sensitivity and range for each case. Optimization in terms of bandwidth and detuning frequency for all configurations aims to achieve higher possible values for the monitoring range and sensitivity.

Some of the obtained results are presents in Fig.16 for OSNR monitoring and Fig.17 for CD monitoring.

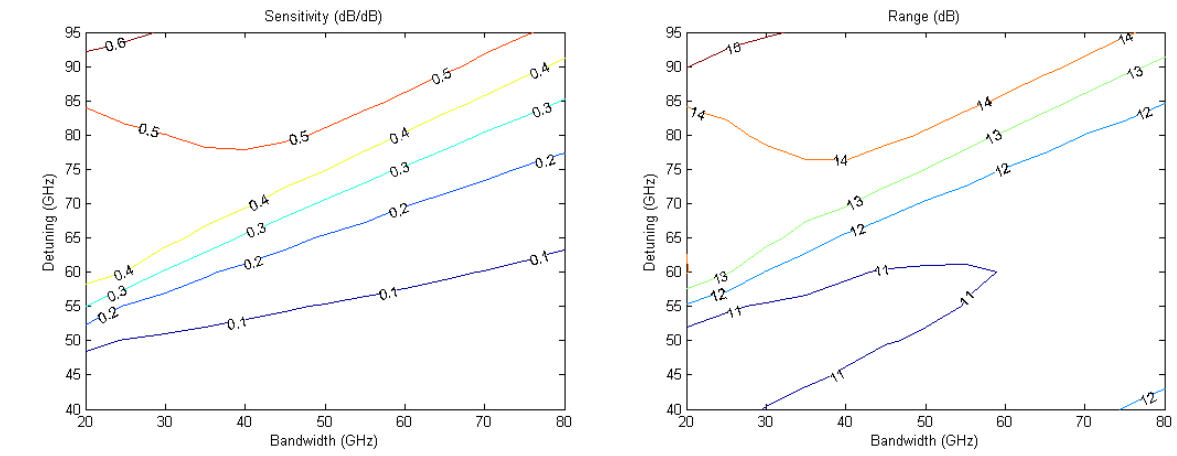

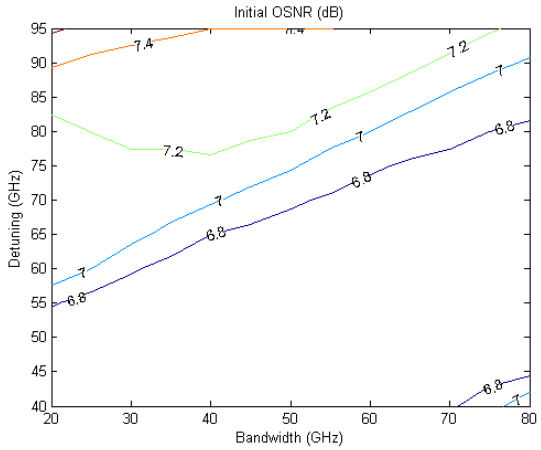

Fig.16 – Optimization results for determining optimal sensitivity (top left), range (top right) and minimum OSNR (down center) of the monitoring OSNR strategy.

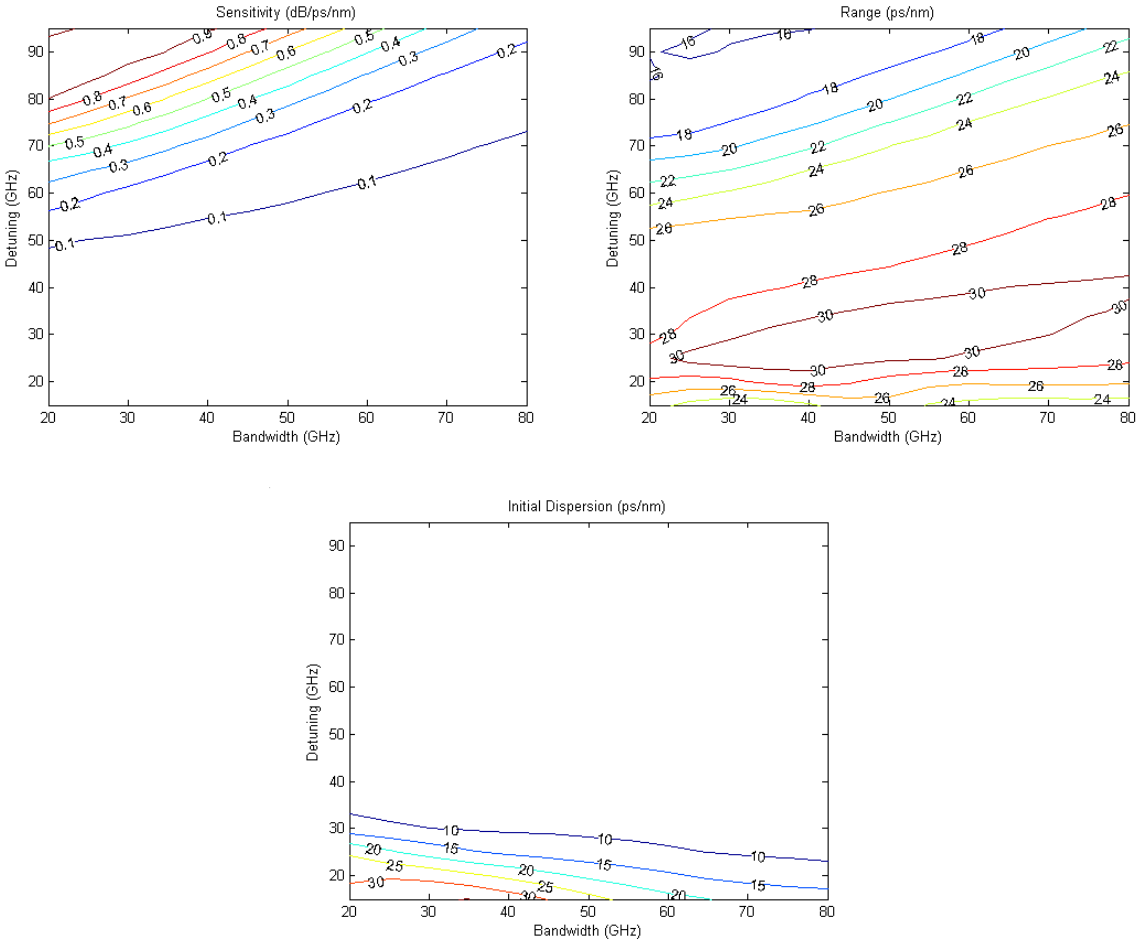

Fig.17– Optimization results for determining optimal sensitivity (top left), range (top right) and minimum accumulated dispersion (down center) of the monitoring CD strategy.

3.2. Simulation results for OSNR monitoring at 40 Gb/s

To have an initial idea of the behavior of the spectrum at the output of the SOA, simulations with an optical analyzer with Gaussian bandwidth resolution 4 GHZ were performed in NRZ modulation format and for two different values of OSNR, as shown in the Fig.18 and Fig.19.

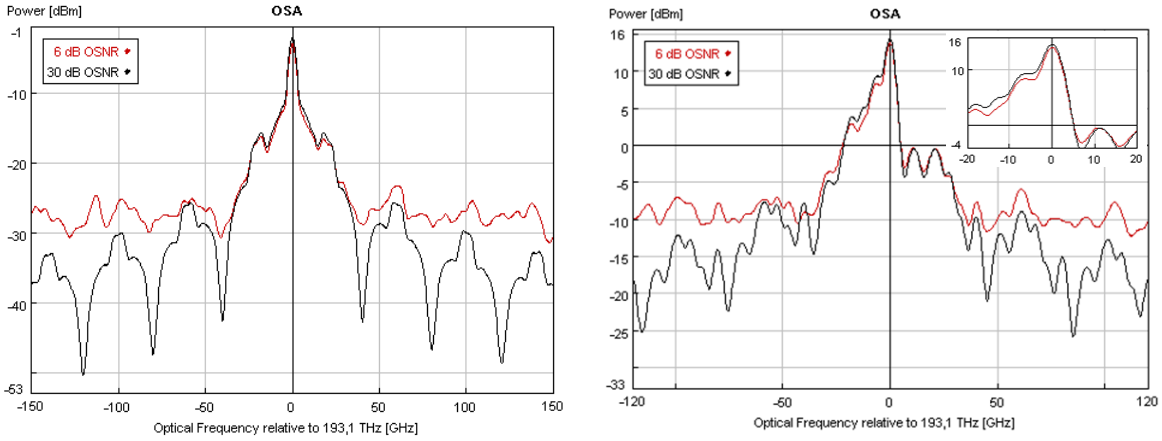

Fig.18 – Output spectrum before SOA (left) and after SOA (right) for SPM without pump for NRZ modulation format.

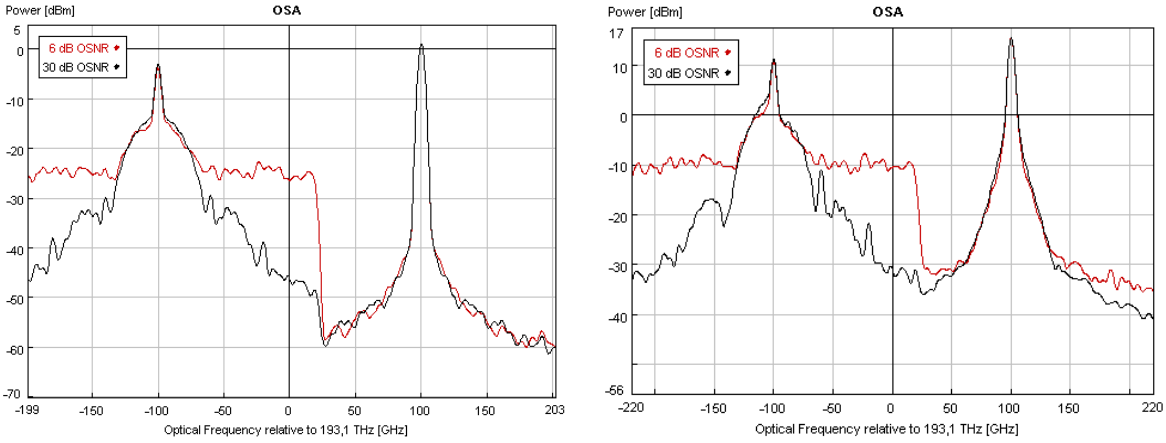

Fig.19 – Output spectrum before SOA (left) and after SOA (right) for SPM with pump and XPM for NRZ modulation format.

Increasing optical noise will increase the spread of pulses amplitudes about the average mark level. Increased pulse amplitudes lead to a larger frequency shifts and, therefore

increased spectral spreading, as observed on the blue side (higher frequency components). Thus, the blue filter is used to OSNR monitoring. However, the red filter is also used, for comparison between blue filter and red filter. On the other hand, the SOA gain saturation effects result in a reduction in the optical power spectral density on the red side (lower frequency components). Note that for SPM without pump, the red side has the opposite dependence on OSNR compared to the blue side, as shown in the magnified view on Fig.18 (right).

As depicts in Fig.19 (right) the XPM effects do not allow OSNR monitoring, due to OSNR mask this effect. Thus, monitoring OSNR based in XPM effect becomes difficult.

3.2.1. Data format dependence

To have an idea of the data format dependence in behavior of the spectrum at the output of the SOA, simulations were performed for three modulation formats and for 30 dBm OSNR, as can be seen in the Fig.20.

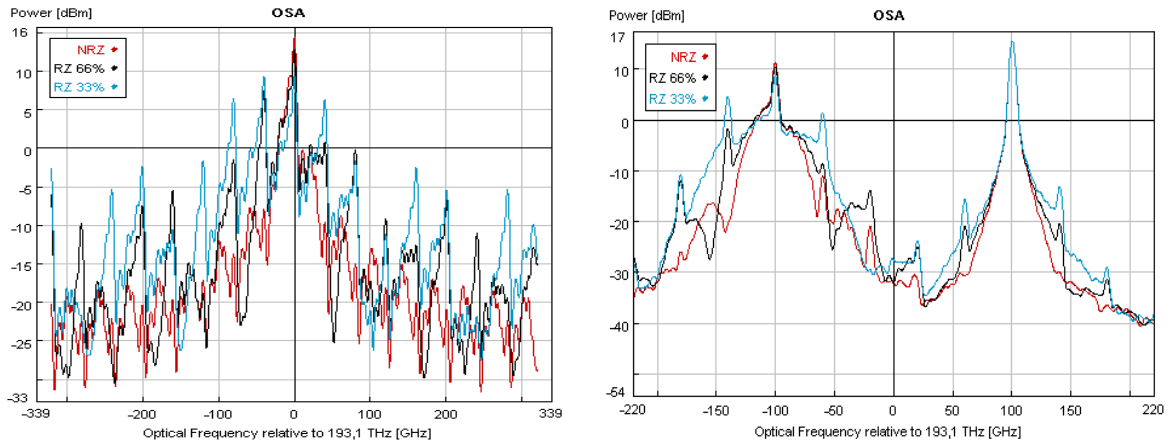

Fig.20 – Output spectrum of the SOA for SPM without pump (left), and for SPM with pump and XPM (right) for NRZ, RZ 66% and RZ 33%.

According the Fig.20, it can be seen that, when increasing the RZ signal duty cycle and for limit case of the NRZ format, the data and pump signal spectra became narrower.

The detuning and bandwidth are given relatively to the data signal and pump signal central frequency. An example is illustrated in Fig.21 for SPM with pump and XPM.

The optimization of optical filter was performed as a way to ease the comparison between blue and red optical filters for both configurations and between different

modulation formats. Signal power stands for the optical power after filtering the components we needed.

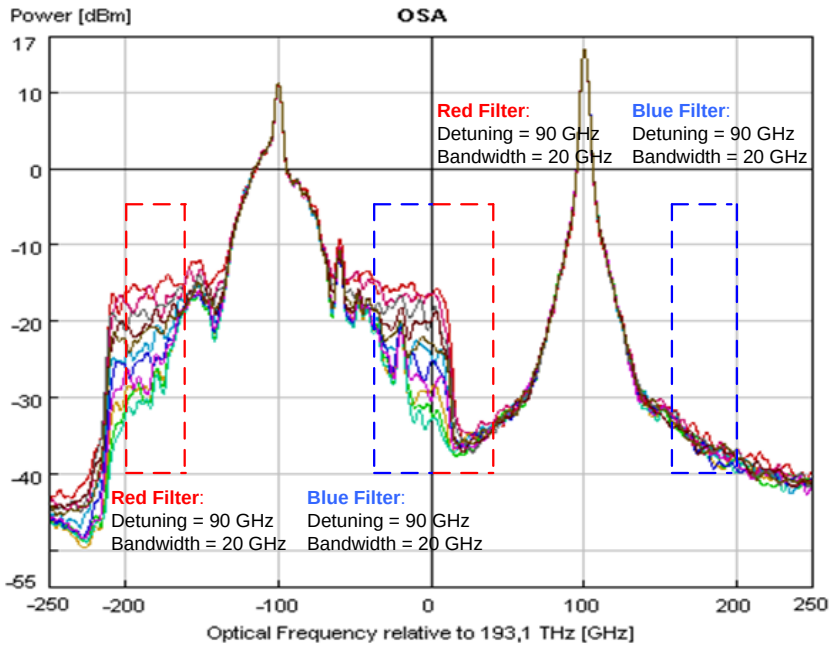

Fig.21 – Illustration of blue and red optical filtering part, 90 GHz detuned and 20 GHz of bandwidth for SPM with pump and XPM.

Fig.22 and Fig.23 show the monitoring signal as the OSNR is varied. Curves are shown for two filters, blue filter (on higher frequency components sides) and red filter (on the lower frequency components side).

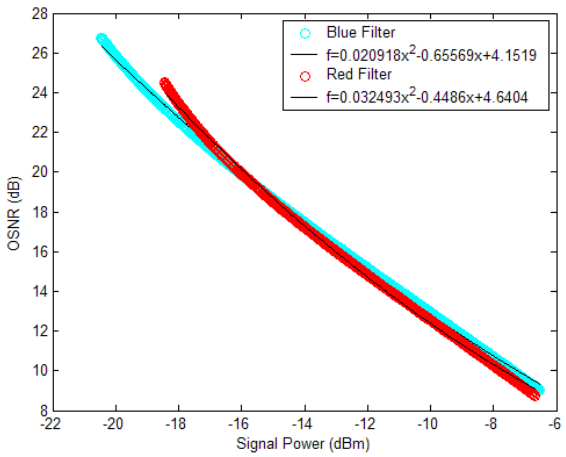

Fig.22 – Monitoring signal for SPM without pump and NRZ modulation format.

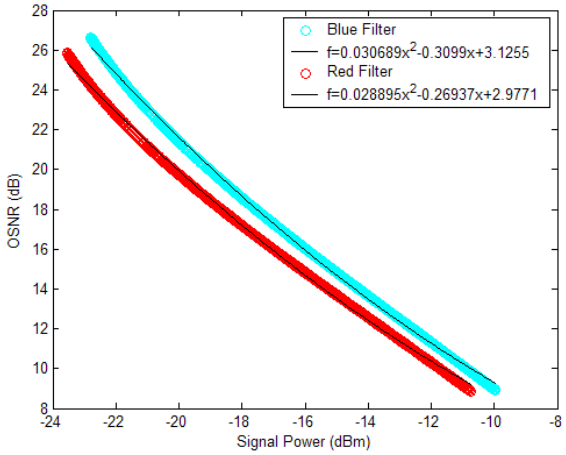

Fig.23 – Monitoring signal for SPM with pump and NRZ modulation format.

Configuration	Optical Filter	Detuning [GHz]	Bandwidth [GHz]	Sensitivity [dB/dB]	Range [dB]
SPM without Pump	Blue Filter	95	20	0.785	17.743
	Red Filter	90	20	0.747	15.741
SPM With Pump	Blue Filter	95	20	0.725	17.693
	Red Filter	95	20	0.753	16.992

Fig.24 – Results for NRZ for both configurations and for both filters.

For both configurations and for both filters, shown in Fig.22 and Fig.23, presented a similar OSNR range and similar sensitivity. However the blue filter for the first configuration presented the best results (~ 0.8 dB/dB sensitivity and ~18 dB range).

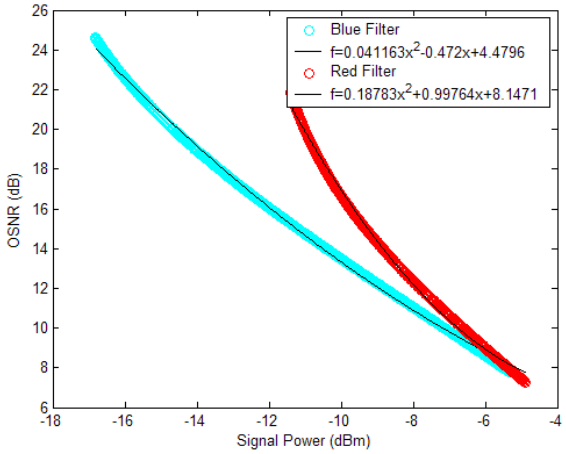

Fig.25 – Monitoring signal for SPM without pump and RZ 66% modulation format.

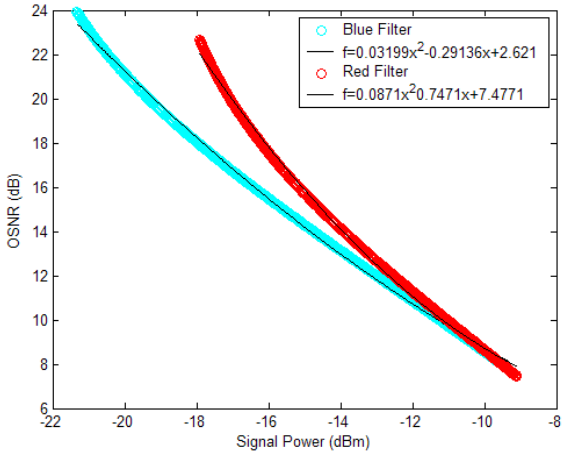

Fig.26 – Monitoring signal for SPM with pump and RZ 66 % modulation format.

Configuration	Optical Filter	Detuning [GHz]	Bandwidth [GHz]	Sensitivity [dB/dB]	Range [dB]
SPM without Pump	Blue Filter	95	20	0.691	16.742
	Red Filter	95	20	0.491	13.113
SPM With Pump	Blue Filter	95	20	0.742	16.116
	Red Filter	95	20	0.579	15.215

Fig.27 – Results for RZ 66% for both configurations and for both filters.

Fig.25 and Fig.26, show that blue filter presents higher range for first configuration (~17 dB) and higher sensitivity for second configuration (~ 0.75 dB/dB). The red filter presents worst results when compared with blue filter.

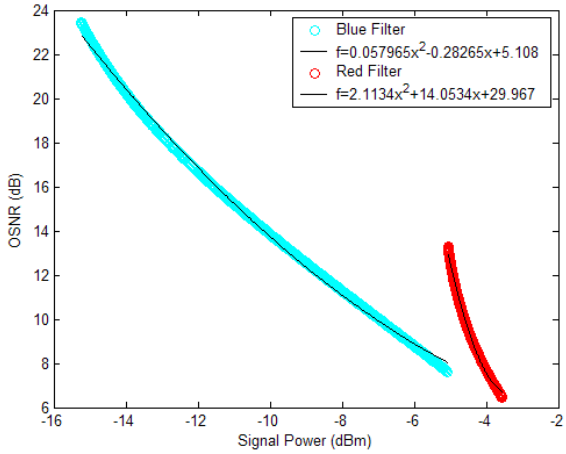

Fig.28 – Monitoring signal for SPM without pump and RZ 33% modulation format.

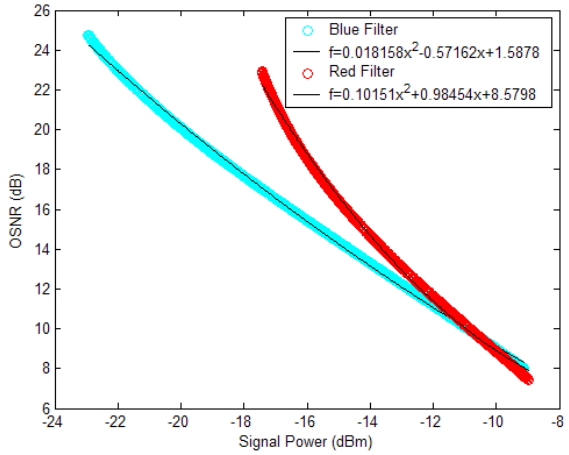

Fig.29 – Monitoring signal for SPM with pump and RZ 33% modulation format.

Configuration	Optical Filter	Detuning [GHz]	Bandwidth [GHz]	Sensitivity [dB/dB]	Range [dB]
SPM without Pump	Blue Filter	95	20	0.642	15.841
	Red Filter	95	20	0.220	6.8569
SPM With Pump	Blue Filter	85	20	0.826	16.742
	Red Filter	95	20	0.547	15.465

Fig.30 – Results for RZ 33% for both configurations and for both filters.

For both configurations, shown in Fig.28 and Fig.29, blue filter presented a similar OSNR range, (~16 dB for SPM without pump and ~17 dB for SPM with Pump). However the sensitivity is higher for the second configuration (~0.8 dB/dB). The red filter is the worst filter, since the sensitivity and range are lower than for blue filter.

In a general way, the blue filter shows a stronger dependence on OSNR and it increases as the noise signal decreases. However the blue filter presented better performance to OSNR monitor, as explain before. On the other hand, for the blue filter, NRZ modulation format presents better results for both configurations. Thus, only NRZ modulation format and optimization with blue filter will be evaluated in experiment.

3.3. Comparison between experimental and simulation results for OSNR monitoring at 40 Gb/s

Taking a measurement of the power on the high frequency side (blue portion) of the spectrum at the output of the SOA, by using the optimal optical filter, chosen by the method described before, it is possible to monitor the degree of OSNR on the optical signal.

Results for the two configurations were obtained in the optimal conditions and fit to a set of 2nd order. These results are shown in Fig.31 and Fig.32.

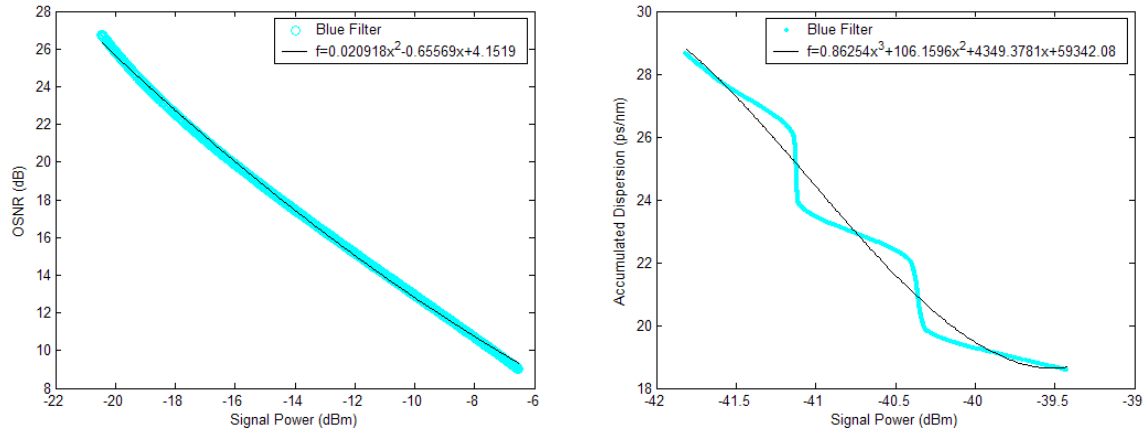

Fig.31 – Simulation (left) and experimental (right) results for SPM without pump for NRZ format.

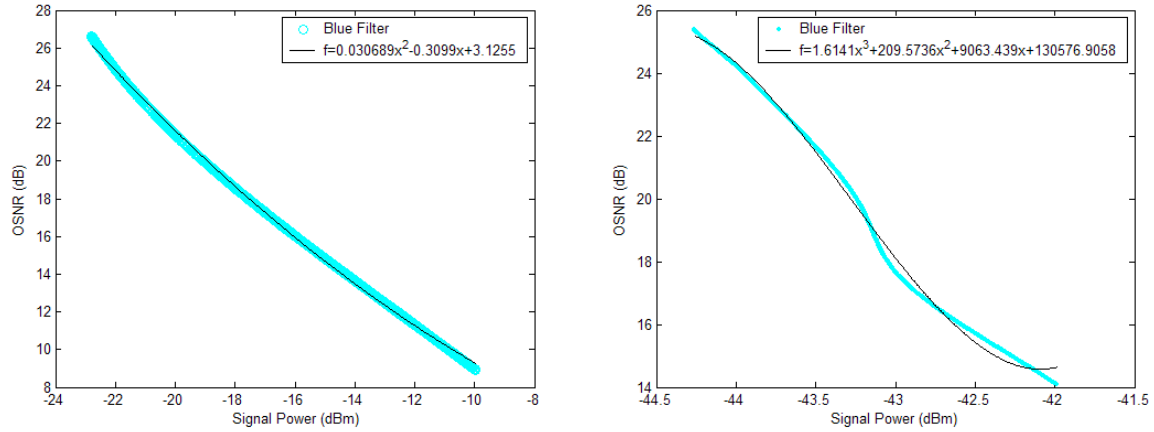

Fig.32– Simulation (left) and experimental (right) results for SPM with pump for NRZ format.

Configuration	Detuning [GHz]	Bandwidth [GHz]	Sensitivity [dB/dB]	Range [dB]
Without Pump	95	20	0.785	17.743
With Pump	95	20	0.725	17.693

Fig.33 – Simulation results for SPM without pump and NRZ modulation format.

Configuration	Detuning [GHz]	Bandwidth [GHz]	Sensitivity [dB/dB]	Range [dB]
Without Pump	45	15	0.237	10.074
With Pump	45	15	0.202	11.282

Fig.34 – Experimental results for SPM without pump and NRZ modulation format.

The sensitivity curves are presented for both configurations. For the first configuration, Fig.31, the linearity of the obtained validity curves is valid up to ~26 dB for simulation results and ~28 dB for experimental. This method allows measuring a minimum OSNR of ~8 dB for simulations results and ~18 dB for experimental results. For the second configuration, Fig.32, the linearity of the obtained validity curves is valid up to ~26 dB for simulation results and ~24 dB for experimental results. The minimum OSNR achieved is ~8 dB for simulation results and ~14 dB for experimental results. Both simulation configurations presented similar results. However, the second configuration, SPM with pump show a better behavior than first configuration for experimental results .The experimental results, revealed lower range of OSNR, due to power source noise limitation as before mentioned.

Through 2^{nd} order polynomials obtained, it is possible to calculate the OSNR for a specific power.

3.4. Simulation results for CD monitoring at 40 Gb/s

To assess of the behavior of the spectrum at the output of the SOA, simulations with an optical spectrum analyzer with Gaussian bandwidth resolution 4 GHz were done for RZ 33% modulation format and for two different values of accumulated dispersion, as shown in the Fig.35 and Fig.36.

It is notable for all cases that for zero accumulated dispersion, the output spectrum of the SOA exhibits larger frequency shift towards the low frequency side and this effect

diminishes when accumulated dispersion increases, due to the reduce peak amplitude of the marks.

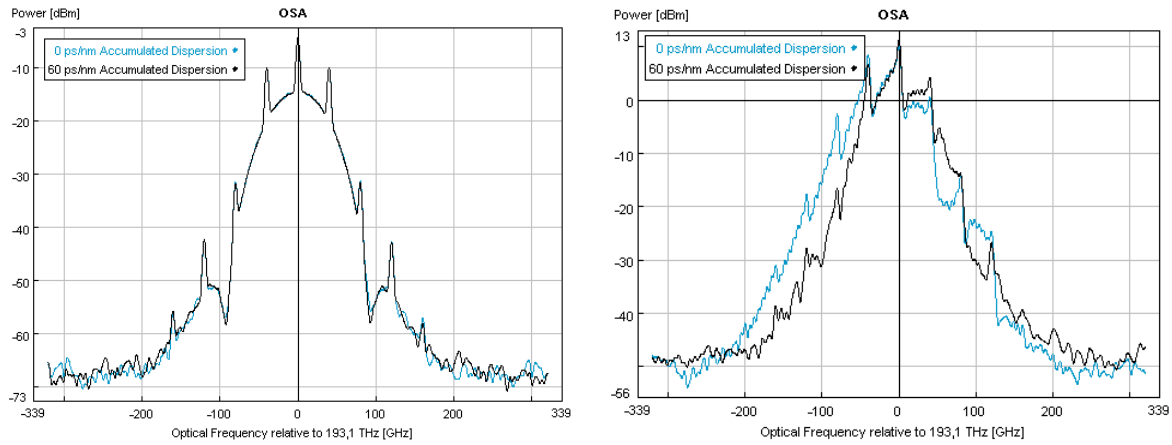

Fig.35 – Output spectrum before SOA (left) and after SOA (right) for SPM without pump for RZ 33%.

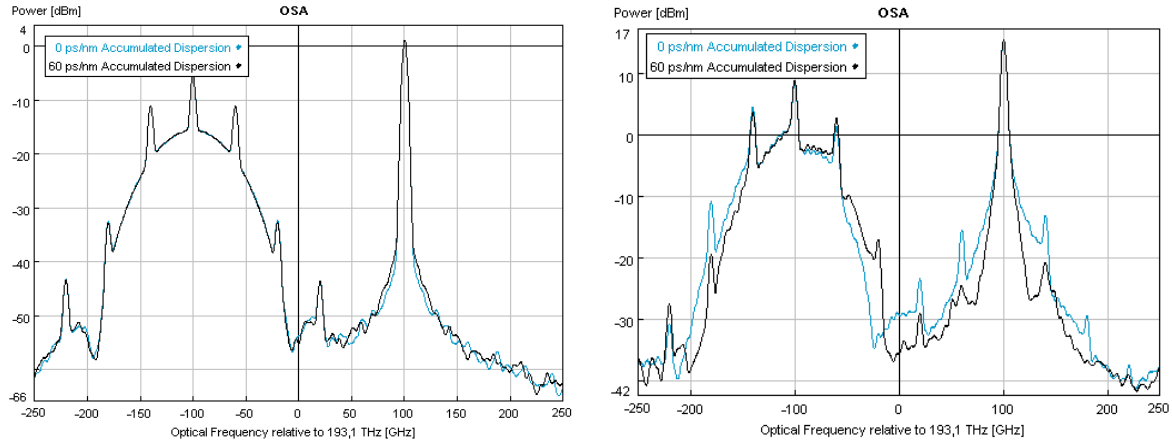

Fig.36 – Output spectrum before SOA (left) and after SOA (right) for SPM with pump and XPM for RZ 33%.

To evaluate the case of negative accumulated dispersion, measurements of the normalized signal power for positive and negative accumulated dispersion were taken with a second Gaussian band pass filter, with 20 GHz bandwidth and detuned 85 GHz from the central frequencies of both SPM and XPM signals at the output of the SOA.

It can be concluded that for both positive and negative dispersion and for all setup configurations, the power of the monitoring signal decreases with increasing accumulated dispersion. It can be observed that, for the case of the SPM without pump, negative

accumulated dispersion measurement loses sensitivity significantly, which can be explained by remembering the following: in the normal dispersion regime, where the dispersion is positive, the lower frequency (or red

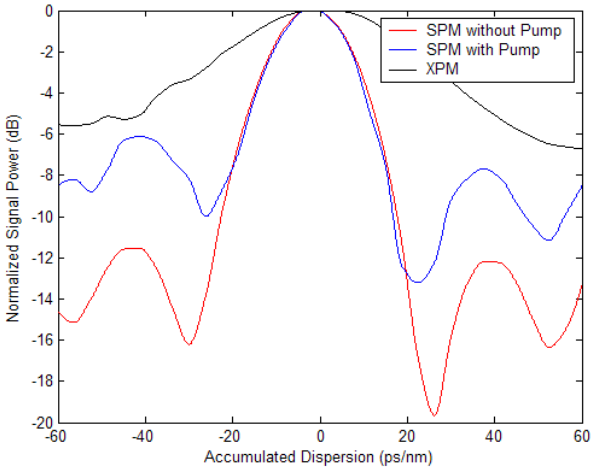

Fig.37 – Normalized signal for negative and positive dispersion and for non-optimized optical filters for SPM without pump, SPM with pump and XPM.

spectral components) components of a pulse travel slower than the blue components, which means that blue components are located in the leading-edge of the pulse. In the opposite case of anomalous dispersion regime, with negative dispersion, the red components of a pulse travel faster than the blue components, so the red components are located in the trailing-edge.

Considering that most of the gain saturation process occurring in the SOA is caused by the leading edge of the pulse, on the anomalous dispersion regime the red components are located closer to the leading-edge of the pulses and the spectral shift effect towards longer wavelengths in the SOA is more pronounced as in the case of the normal dispersion regime. Thus, for the SPM without pump monitoring curve, where the effects of the chirp of the signal and the chirp produced by the SOA are taken into account, different amounts of red-spectral shift of the spectrum at the output of the SOA are obtained for the same absolute value of both positive and negative accumulated dispersion.

The monitoring signal for the XPM case is more symmetrical around the zero dispersion point, because, for this case, the monitoring signal is only dependent on the chirp produced by the SOA, thus having almost the same monitoring power for equal amounts of accumulated dispersion with different sign.

3.4.1. Data format dependence

To have an idea of the data format influence in behavior of the spectrum at the output of the SOA, simulations were done for three modulations format, as illustrated in Fig.38.

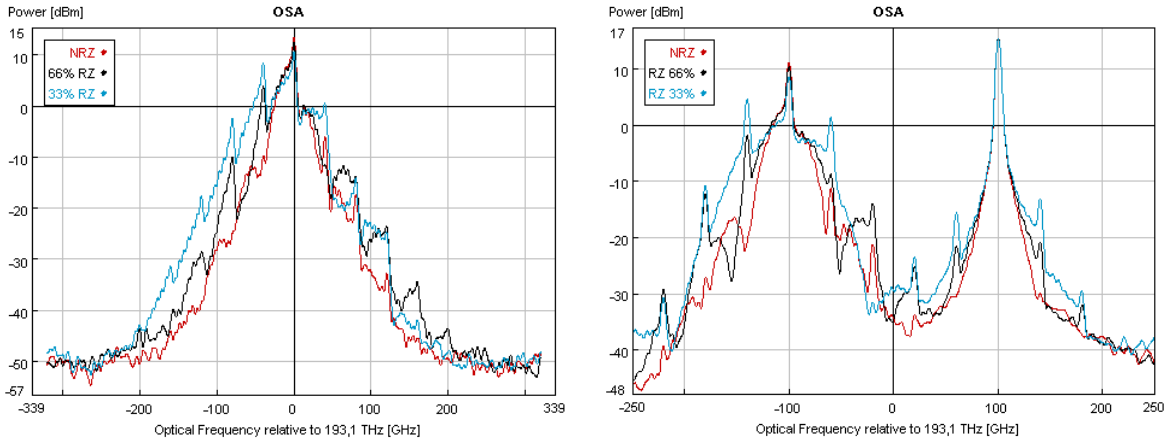

Fig.38– Output spectrum of the SOA for SPM without pump (left), and for SPM with pump and XPM (right) for NRZ, RZ 66% and RZ 33%.

According to Fig.38, when the RZ signal duty cycle increases and for limit case of NRZ format, the data and pump signal spectra become narrower and the frequency components near the optical carrier have higher power, which leads to a decrease of the quality of monitoring signal.

3.4.1.1. Positive Dispersion

The optical filters were once again optimized as a way to facilitate the comparison between different modulation formats, as shown in the Figs.39, 41 and 43. Note that, the minimum dispersion for NRZ is lower than for the cases 33% RZ and 66% RZ. This occurs, because the applied methodology described in Fig.14. This not means that only dispersions higher than e.g.35 ps/nm (NRZ) can be monitorized. This means better compromise between dispersion range and power sensitivity is achieved.

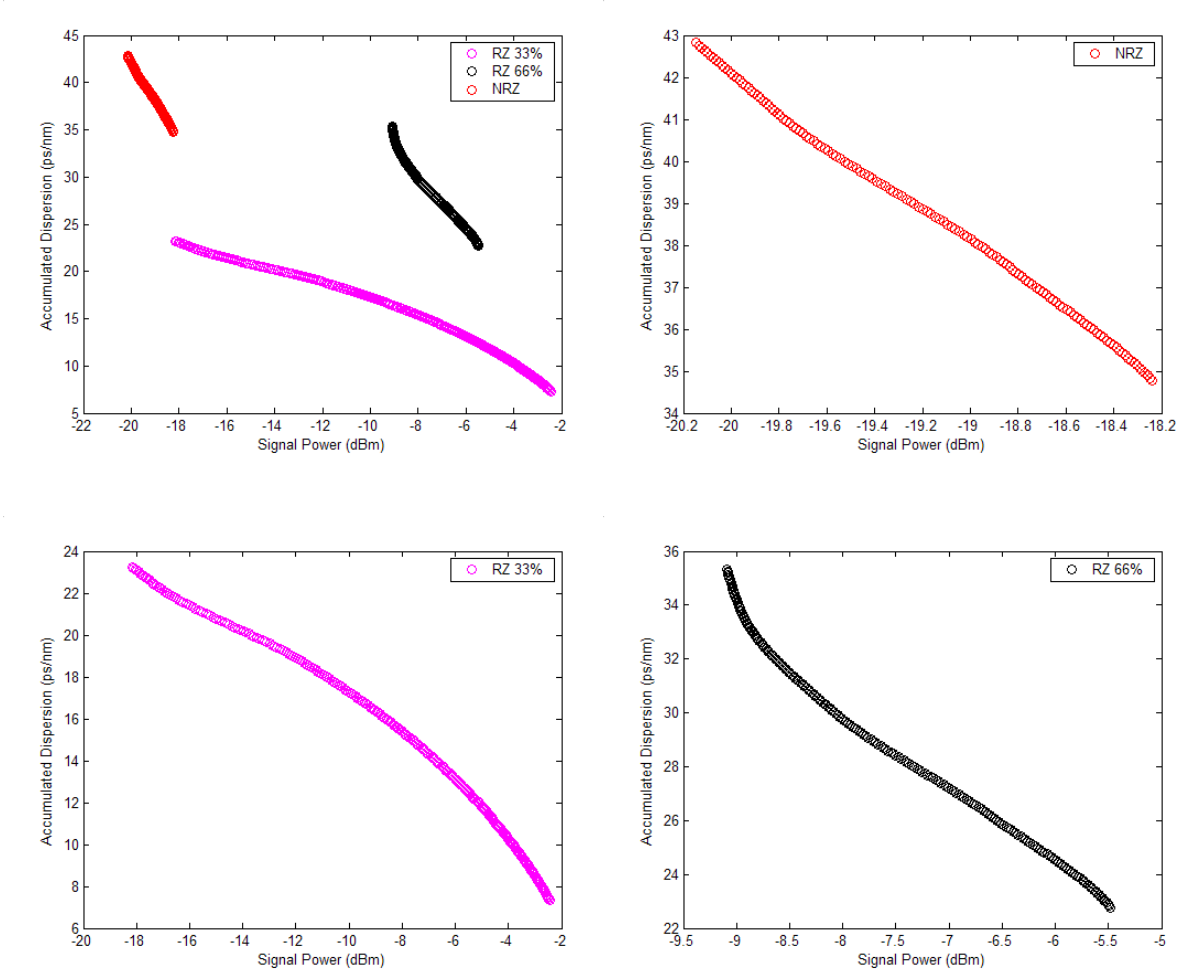

Fig.39 – Monitoring signal for RZ 33%, RZ 66% and NRZ data formats for SPM without pump for optimized filter.

Configuration	Detuning [GHz]	Bandwidth [GHz]	Sensitivity [dB/ps/nm]	Range [ps/nm]
RZ 33%	85	20	0.987	15.916
RZ 66%	85	20	0.288	12.553
NRZ	95	25	0.237	8.048

Fig.40 – Results for SPM without pump for RZ 33%, RZ66% and NRZ modulation formats.

For first configuration (SPM without pump), the Fig.39 show that RZ 33% modulation format presented higher accumulated dispersion range (~16 ps/nm) and higher sensitivity (~ 0.99 dB/ps/nm).

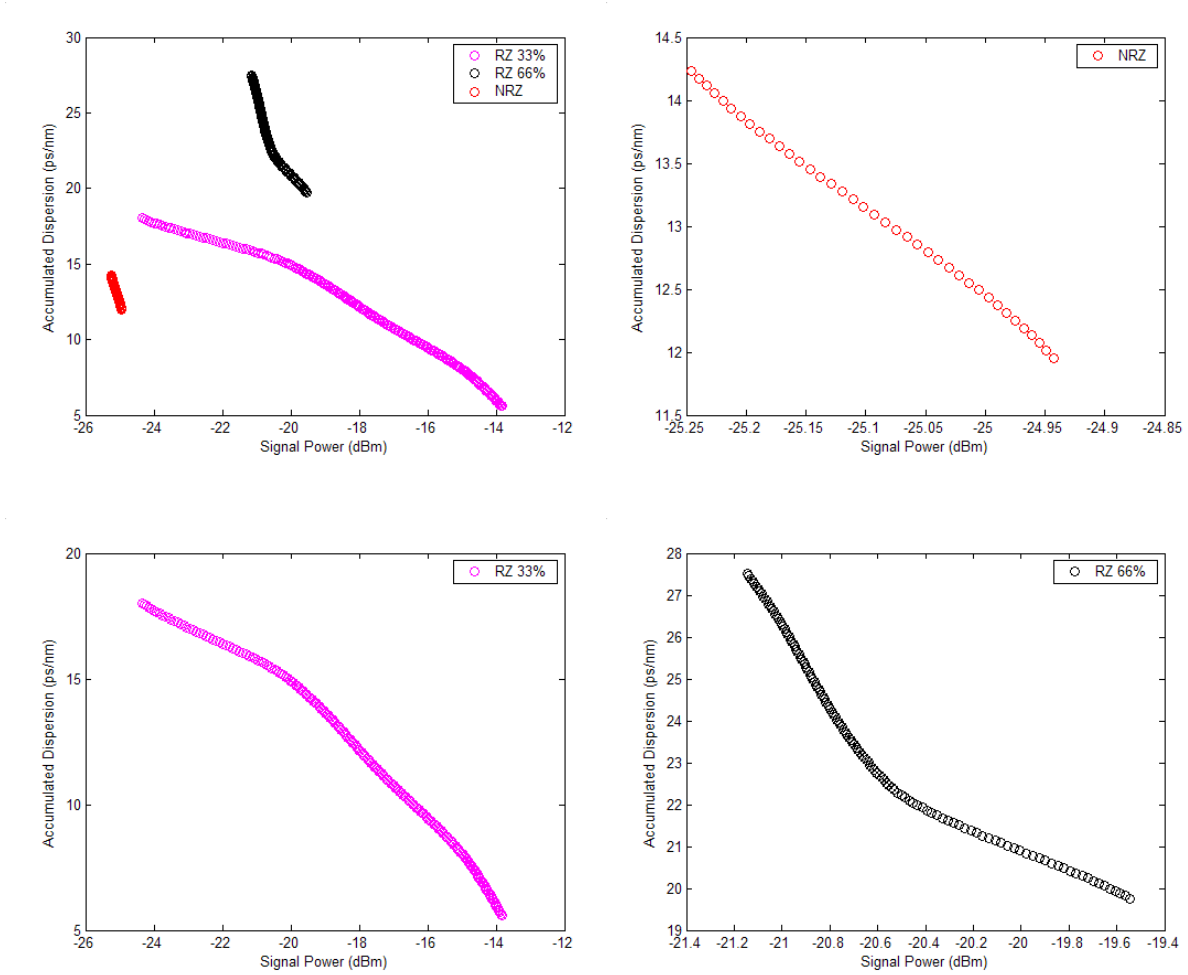

Fig.41 – Monitoring signal for 33% RZ, 66% RZ and NRZ data formats for SPM with pump for optimized higher sensitivity filter.

Configuration	Detuning [GHz]	Bandwidth [GHz]	Sensitivity [dB/ps/nm]	Range [ps/nm]
RZ 33%	90	20	0.846	12.432
RZ 66%	95	20	0.207	7.748
NRZ	95	20	0.133	2.282

Fig.42 – Results for SPM with pump for RZ 33%, RZ66% and NRZ modulation formats.

For the case of second configuration (SPM with pump), the Fig.41 depicts that RZ 33% modulation format presented higher accumulated dispersion range (~12.4 ps/nm) and higher sensitivity (~0.85 dB/ps/nm).

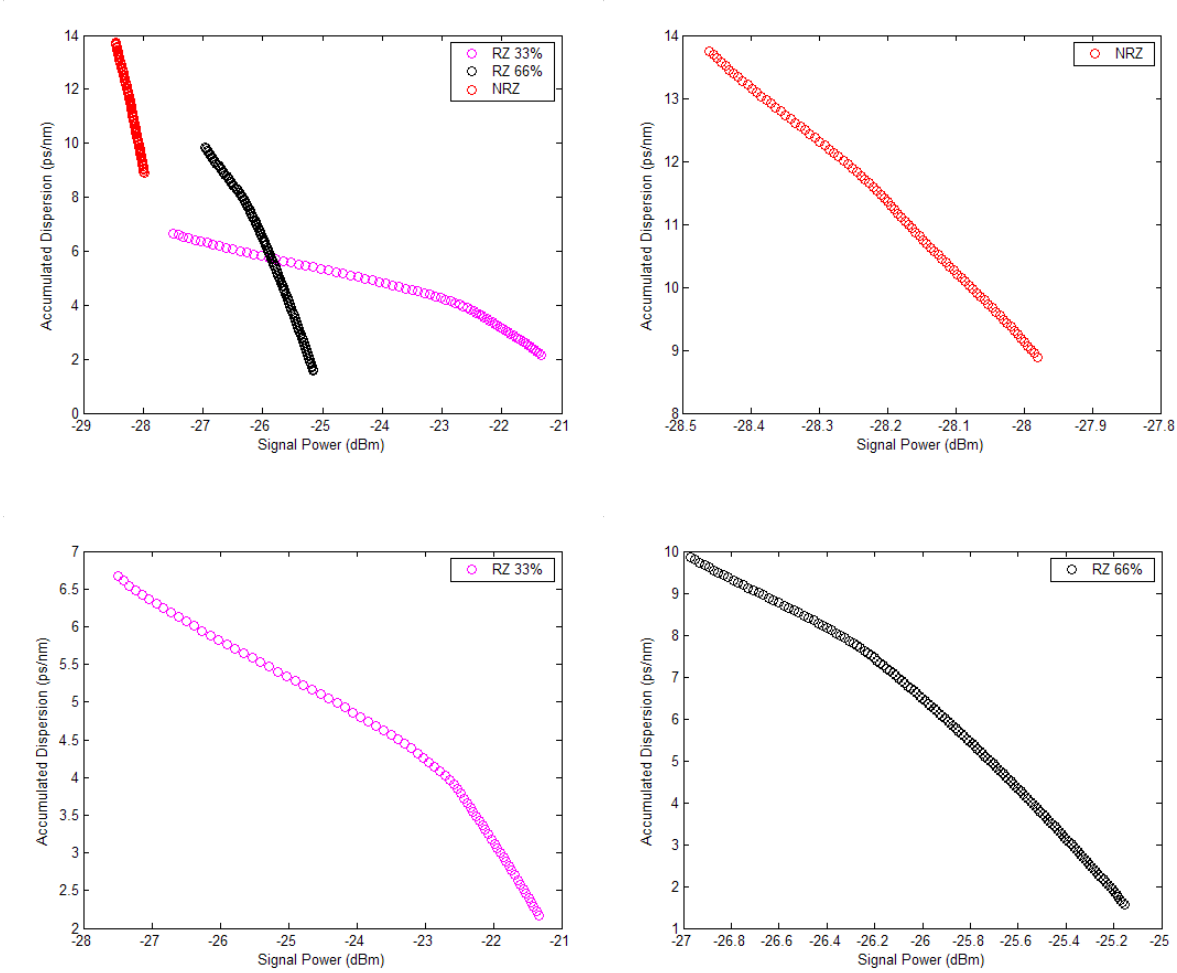

Fig.43 – Monitoring signal for 33% RZ, 66% RZ and NRZ data formats for XPM for optimized higher sensitivity filter.

Configuration	Detuning [GHz]	Bandwidth [GHz]	Sensitivity [dB/ps/nm]	Range [ps/nm]
RZ 33%	85	20	1.369	4.505
RZ 66%	95	20	0.219	8.288
NRZ	70	20	0.099	4.865

Fig.44 – Results for XPM for RZ 33%, RZ66% and NRZ modulation formats

For the case of second configuration (XPM), the Fig.43 depicts that RZ 33% modulation format presents higher sensitivity (~1.4 dB/ps/nm), however presents worst accumulated dispersion range (~ 5 ps/nm).

Can be concluded, that RZ 33% is better modulation format to monitoring positive

dispersion, due better compromise between sensitivity range compared with others modulation formats. For this reasons, only RZ 33% modulation format will be evaluated in experimentally for both positive and negative dispersion.

On the other hand, the first configuration (SPM without pump) exhibits better compromise between sensitivity and range.

3.5. Comparison between experimental and simulation results for CD monitoring at 40 Gb/s

Taking a measurement of the power of the low frequency side of the spectrum at the output of the SOA, by using the optimal optical filter, it is possible to monitor the degree of accumulated dispersion on the optical signal.

As done previosly for monitoring OSNR, the results for the two configurations, as shown in the Fig.45-56, were obtained in the optimal conditions and fit to a set of 2nd order polynomials.

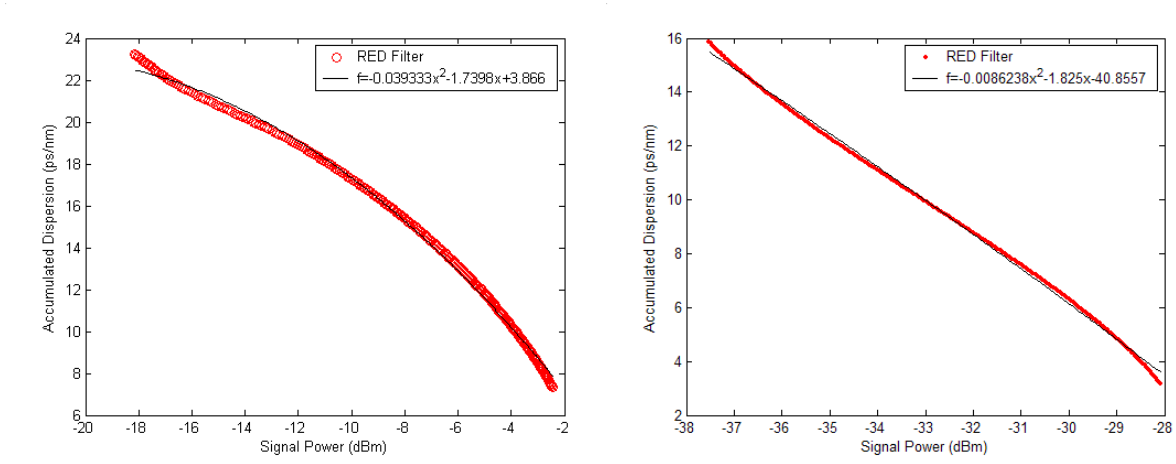

Fig.45 – Simulation (left) and experimental (right) results for SPM without pump, RZ 33% format and positive dispersion.

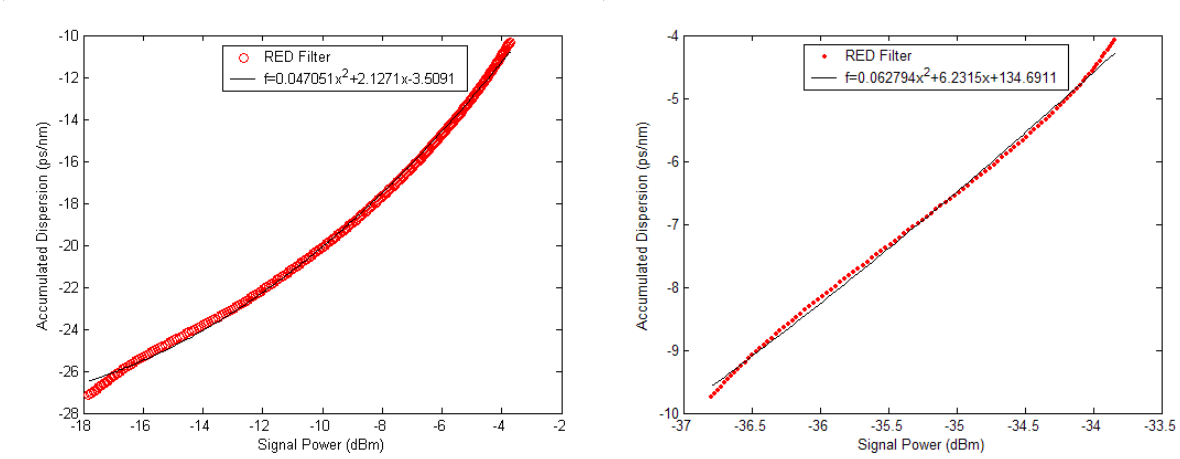

Fig.46 – Simulation (left) and experimental (right) results for SPM without pump, RZ 33% modulation format and negative dispersion.

	Detuning [GHz]	Bandwidth [GHz]	Sensitivity [dB/ps/nm]	Range [ps/nm]
Positive Dispersion	85	20	0.987	15.916
Negative Dispersion	90	20	0.839	16.817

Fig.47 – Simulation results for SPM without pump and RZ 33% modulation format.

	Detuning [GHz]	Bandwidth [GHz]	Sensitivity [dB/ps/nm]	Range [ps/nm]
Positive Dispersion	35	5	0.745	12.673
Negative Dispersion	5	5	0.519	5.671

Fig.48 – Experimental results for SPM without pump and RZ 33% modulation format.

The simulation and experimental sensitivity curves for dispersion monitoring based in SPM (without pump) are presented in Fig.45 and Fig.46 for positive and negative accumulated dispersion respectively. The linearity of the obtained validity curves for positive dispersion is valid up to ~22 ps/nm for simulation and up to ~15 ps/nm for experiment. The validity curves for negative dispersion is valid up to ~−12 ps/nm for simulation and up to ~ −5 ps/nm for experiment. With this method it is possible to measure the positive accumulated dispersion minimum of ~6 ps/nm for simulations results and ~2 ps/nm for experimental results, and for negative accumulated dispersion of ~ −28 ps/nm for simulation results and ~ −10 ps/nm for experimental results. Both positive and

negative dispersions present a similar monitoring sensitivity and range. However for experimental results the monitoring range is lower for negative dispersion.

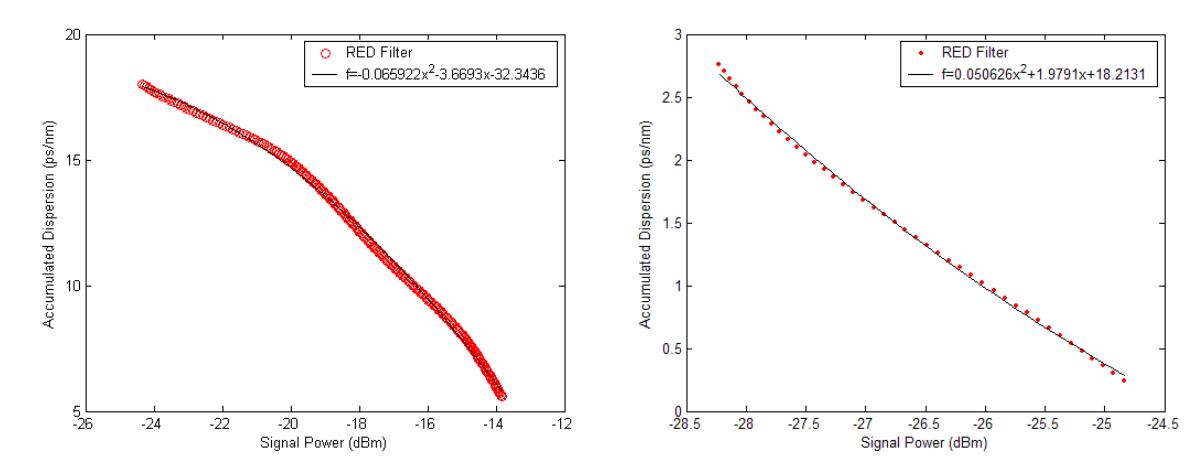

Fig.49 – Simulation (left) and experimental (right) results for SPM with pump, RZ 33% format and positive dispersion.

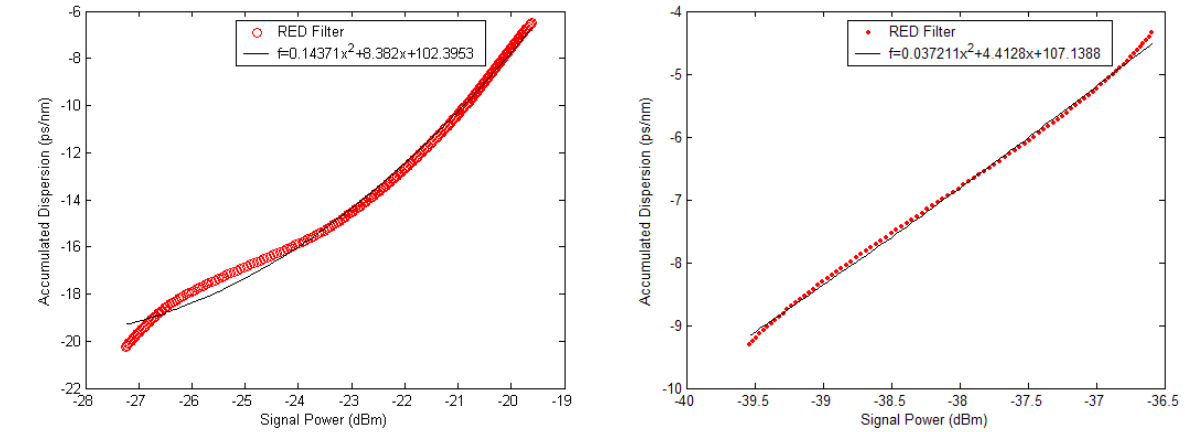

Fig.50 – Simulation (left) and experimental (right) results for SPM with pump, RZ 33% format and negative dispersion.

	Detuning [GHz]	Bandwidth [GHz]	Sensitivity [dB/ps/nm]	Range [ps/nm]
Positive Dispersion	90	20	0.846	12.432
Negative Dispersion	95	20	0.555	13.754

Fig.51 – Simulation results for SPM with pump and RZ 33% modulation format.

	Detuning [GHz]	Bandwidth [GHz]	Sensitivity [dB/ps/nm]	Range [ps/nm]
Positive Dispersion	40	5	1.344	2.523
Negative Dispersion	10	5	0.595	4.955

Fig.52 – Experimental results for SPM with pump and RZ 33% modulation format.

The simulation and experimental sensitivity curves for dispersion monitoring based in SPM (with pump) are presented in Fig.49 and Fig.50. The linearity of the obtained validity curves for positive dispersion is valid up to ~17 ps/nm for simulation and up to ~2.5 ps/nm for experiment. The validity curves for negative dispersion is valid up to ~−8 ps/nm for simulation and up to ~−5 ps/nm for experiment. With this method is possible to measure the minimum positive accumulated dispersion of ~5 ps/nm for simulation results and ~0.5 ps/nm for experimental results and for negative accumulated dispersion of ~ −20 ps/nm for simulation results and ~ − 9 ps/nm for experimental results. The two accumulated dispersions present different sensitivity and range. The positive accumulated dispersion presents higher sensitivity (~0.85 dB/ps/nm for simulations and 1.34 dB/ps/nm for experiment) and negative accumulated dispersion presents higher range (~14 ps/nm for simulations and ~5 ps/nm for experiment).

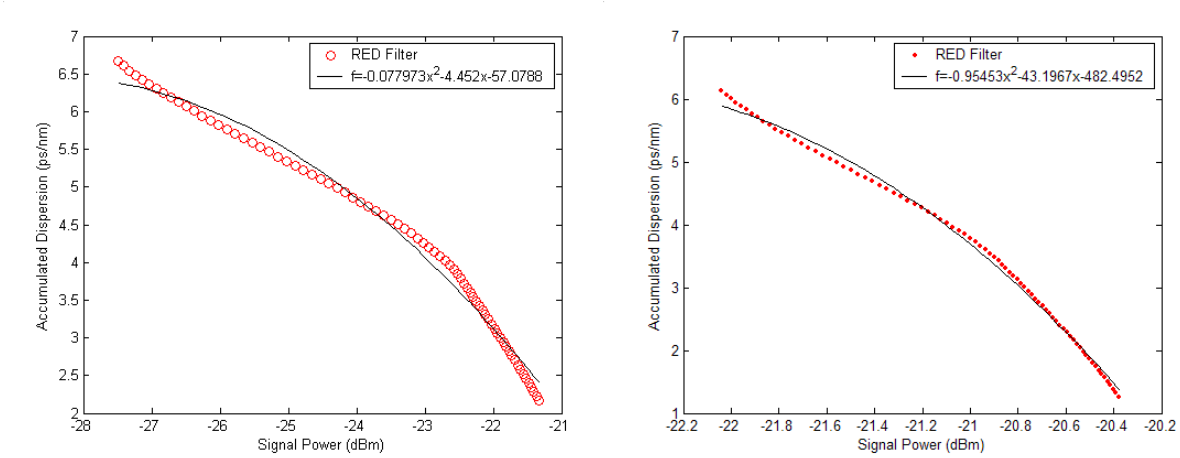

Fig.53 – Simulation (left) and experimental (right) results for XPM, 33% RZ format and positive dispersion.

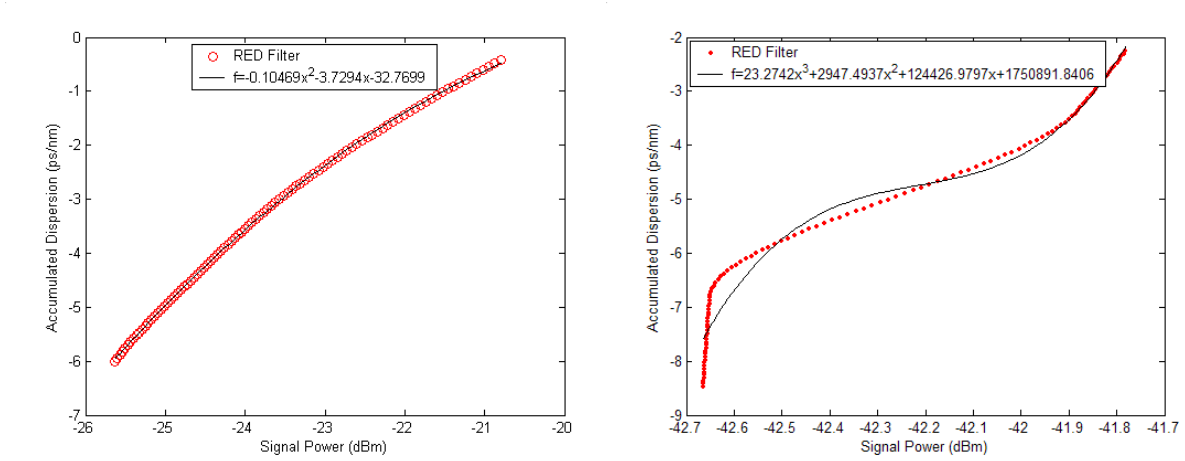

Fig.54 – Simulation (left) and experimental (right) results for XPM, RZ 33% format and negative dispersion.

	Detuning [GHz]	Bandwidth [GHz]	Sensitivity [dB/ps/nm]	Range [ps/nm]
Positive Dispersion	85	20	1.369	4.505
Negative Dispersion	80	25	0.866	5.586

Fig.55 – Simulation results for XPM and 33% RZ modulation format.

	Detuning [GHz]	Bandwidth [GHz]	Sensitivity [dB/ps/nm]	Range [ps/nm]
Positive Dispersion	5	20	0.341	4.865
Negative Dispersion	5	5	0.142	6.221

Fig.56 – Experimental results for XPM and RZ 33% modulation format.

The simulation and experimental sensitivity curves for dispersion monitoring based in XPM are presented in Fig.53 and Fig.54. The linearity of the obtained validity curves for positive dispersion is valid up to ~6 ps/nm for simulation and experiment. The validity curves for negative dispersion is valid up to ~ -6 ps/nm for simulation and up to ~ -8 ps/nm for experiment. With this method is possible to measure the positive accumulated dispersion minimum of ~2 ps/nm for simulations and experimental results, and for negative accumulated dispersion of ~ -6 ps/nm for simulation and ~ -8 ps/nm for experimental results. Positive accumulated dispersion presents higher sensitivity (~1.37 dB/ps/nm for simulations and 0.34 dB/ps/nm for experiment) and negative accumulated dispersion presents higher range (~5.6 ps/nm for simulations and ~6.2 ps/nm for experiment.

For the results before mentioned, it can be concluded that monitoring based in SPM (without pump) for simulation results presents better compromise between monitoring dispersion range and sensitivity. For simulation results, monitoring dispersion range corresponds to ~16 ps/nm and sensitivity to ~0.99 dB/ps/nm for positive accumulated dispersion, and to ~17 ps/nm of monitoring dispersion range and ~0.84 dB/ps/nm of sensitivity for negative dispersion. The experimental results also present better compromise for SPM (without pump). The monitoring dispersion range is ~13ps/nm and ~5.7 ps/nm for positive and negative dispersion respectively. The sensitivity corresponds to ~0.75 dB/ps/nm and to ~0.5 dB/ps/nm for positive and negative dispersion, respectively

Thus, with the 2^{nd} order polynomials obtained, it is possible to calculate the accumulated dispersion inside the monitoring range.

3.6. References

1. P. Vorreau, D. C. Kilper, J. Leuthold, "Optical Noise and Dispersion Monitoring with SOA-Based Optical 2R Regenerator", IEEE Photon. Technol. Lett., Vol. 17, No. 1, Jan. 2005.

2. Y. Shi, M. Chen, S. Xie, “A novel low power chromatic dispersion monitoring technique employing SOA spectral shift”, Optics Communications, Vol. 230, pp. 297-300, Nov. 2003.

3. VPI Photonics Modules Reference Manual, FilterOpt, 2008.

CHAPTER 4

Conclusions and Future Work

Two variants of a technique for optically monitoring the OSNR and CD were presented and characterized: SPM and XPM in SOAs. It has been shown that measuring the spectral red-shift effect variation on a SOA for different amounts of accumulated dispersion constitutes a simple technique to monitor CD with high values of monitoring sensitivity and range. On the other hand, measuring the spectral broadening in the blue side with the noise increases it is possible to monitor OSNR. The dependence of the blue shift on OSNR may provide the opportunity to distinguish between noise and dispersion. In a such way, to monitor simultaneous OSNR and CD, two filters will be necessary, blue filter (higher frequency components) and red filter (lower frequency components) respectively.

Using this technique, it has been seen that is possible to correctly monitor the OSNR with a monitoring sensitivity of about 0.8 dB/dB and monitoring range of 18 dB (OSNR ~8 dB to ~26 dB) for simulation, and with a monitoring sensitivity of about 0.2 dB/dB and monitoring range 11 dB in the experimental (OSNR ~14 dB to ~25 dB).

For monitoring CD is possible to correctly monitor the amount of positive accumulated dispersion with a monitoring sensitivity of about 0.99 dB/ps/nm and a monitoring range of about 16 ps/nm (CD ~8 ps/nm to ~23 ps/nm) for simulations, and with a monitoring sensitivity of about 0.75 dB/ps/nm and monitoring range of about 13 ps/nm in the experiment (CD ~ 3 ps/nm to ~16 ps/nm). For negative accumulated dispersion was obtained a monitoring sensitivity of about 0.84 dB/ps/nm and a monitoring range of about 17 ps/nm (CD ~ −27 ps/nm to ~ −10 ps/nm) for simulations, and with a monitoring sensitivity of about 0.52 dB/ps/nm and monitoring range of about 5.7 ps/nm in the experiment (CD ~ −10 ps/nm to ~ −4 ps/nm).

A set of 2nd order polynomials well suitable was implemented for OSNR and CD. Thus in a very inexpensive hardware after the photo detection, e. g. low cost microcontroller, it is possible to monitor OSNR and CD.

A simultaneous and independent optical performance monitoring for CD and OSNR is desirable and will be addressed in future work.